WILEY-VCH

Challenges and Opportunities of Self-healing Polymers and Devices for Extreme and Hostile Environments

James Ekeocha[1], Christopher Ellingford[1], Min Pan[2], Alan M Wemyss[1], Christopher Bowen[2], Chaoying Wan[1]**

James Ekeocha, Christopher Ellingford, Dr. Alan M Wemyss, Dr. Chaoying Wan
[1]International Institute for Nanocomposites Manufacturing (IINM), WMG, University of Warwick, CV4 7AL, UK
E-mail: chaoying.wan@warwick.ac.uk

Dr. Min Pan, Prof. Christopher Bowen
[2] Department of Mechanical Engineering, University of Bath, BA2 7AY, UK
Email: msscrb@bath.ac.uk

Keywords: self-healing, polymer, composite, device, extreme environment

Abstract

Engineering materials and devices can be damaged during their service life as a result of mechanical fatigue, punctures, electrical breakdown and electrochemical corrosion. This damage can lead to unexpected failure during operation, which requires regular inspection, repair and replacement of the products, resulting in additional energy consumption and cost. During operation in challenging, extreme or harsh environments, such as those encountered in high or low temperature, nuclear, offshore, space, and deep mining environments, the robustness and stability of materials and devices are extremely important. Over recent decades, significant effort has been invested into improving the robustness and stability of materials through either structural design, the introduction of new chemistry, or improved manufacturing processes. Inspired by natural systems, the creation of self-healing materials has the potential to overcome these challenges and provide a route to achieve dynamic repair during service. Current research on self-healing polymers remains in its infancy, and self-healing behaviour under harsh and extreme conditions is a particularly untapped area of research. Here, we discuss the self-healing mechanisms and performance of materials under a variety of harsh

environments. An overview of polymer-based devices developed for a range of challenging environments is provided, along with areas for future research.

1. Introduction

Materials, structures and devices often need to operate in extreme or harsh environments, in applications such as nuclear, offshore, industrial plants, space, and deep mining. *Extreme* conditions typically refers to temperatures outside the range -40 to 125 °C, low or high pressure (such as a vacuum or 200 bar, respectively), intense levels of radiation, shock and vibration, high electric or magentic fields, saturated salt concentrations, highly acidic or alkaline environments (*pH* ~ <2 or >11), and corrosive environments.[1] The materials, components and devices that operate in such conditions need to be sufficiently robust and durable in order to maintain their performance and sustain the harsh working conditions. Furthermore, for challenging areas that are difficult to reach, such as oil fields, the deep ocean, or remote locations, it is desirable for materials to be self-sensing, adaptive, self-healing and perform autonomously, which can prevent people from working in potentially harmful operations, whilst saving energy and reducing operational costs.

Most polymers are electrically or thermally insulating, and thermally stable in a temperature range of -80 and 300 ºC. These characteristics allow polymers to sustain chemical, mechanical, thermal, electrical, or radiation exposure to some extent. Beyond these normal conditions, a new environment that pushes the capabilities of these materials to their limits can be considered as a *harsh* environment, which raises new challenges for developing high performance polymers and devices, including the introduction of *self-healing*. Self-healing polymers refer to materials that are able to recover their structure and properties partially or fully after damage. Therefore, the ability to self-heal provides these materials with the potential for improved reliability, stability and durability.

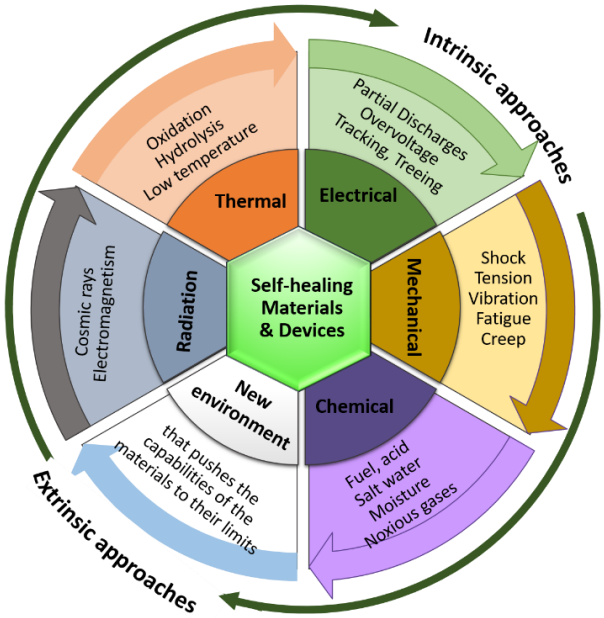

Figure 1. Potential applications of self-healing materials and devices for a range of extreme environments.

An example of a challenging environment is the sealing or adhesive materials used for proton exchange membrane (PEM) fuel cells, which are exposed to acidic liquid solutions, high humidity (up to 100% relative humidity), hydrogen gas, coolants (e.g. synthetic hydrocarbons, perfluorocarbons, fluorosilicone fluids), large temperature cycles (between -40 and 100 °C), electrochemical environments and mechanical stresses. During operation, any gas or fluid leakage between the components due to the degradation of the seals and adhesives can damage the fuel cells and lead to safety concerns; however, there are many other examples. Figure 1 provides a snapshot of the types of difficulties experienced by materials within a variety of extreme environments. The aim of this review is to overview the current technologies that exploit self-healing materials and devices to operate in such conditions, and their current limitations and directions for future development.

2. Self-healing mechanisms of polymers and composites

Self-healing materials are classified into two categories: *extrinsic* and *intrinsic* self-healing. The extrinsic self-healing process relies on the introduction of pre-embedded healing agents, often carried in microcapsules or microvascular fibres, which act to release the healing agents upon rupture and react to bind damaged surfaces. Microcapsules are limited to the infilling of microscopic cracks and the healing process only takes place in locations where fractured capsules are present. Microvascular materials are able deliver more healing fluid than capsules, due to the supply of healing agents by a microvascular network that allows repair of repeated damage and restoration of larger volumes. The strategies used to achieve extrinsic healing are summarised in Figure 2, which shows the range of capsule-assisted and microvascular assisted approaches; the mechanisms have been discussed in detail in recent excellent reviews.[2],[3] However, extrinsic approaches are irreversible, and the embedding of microcapsules or microvascular materials raise further technical challenges for balancing processing, interfaces, mechanical and other functional properties of the composites.

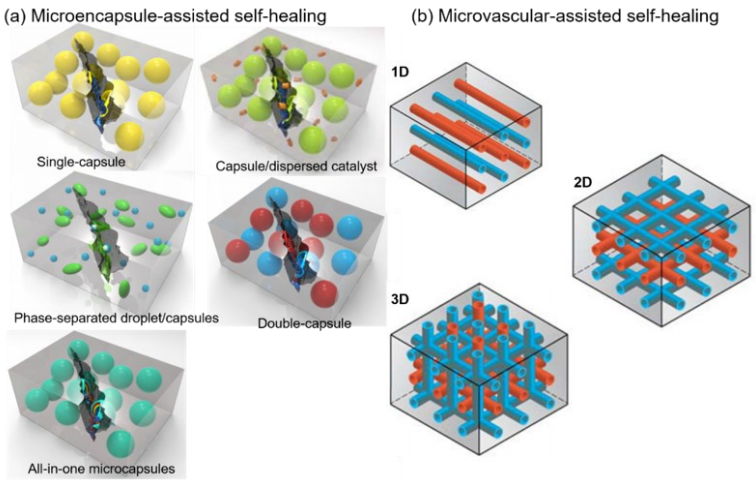

Figure 2 Extrinsic healing approaches (a) Typical self-healing systems based on microcapsules, the healing agent (monomer) can be loaded in single capsule, or additional catalyst is loaded

in a second capsule (double-capsule), or both are loaded in the core and shell wall of the same capsule (all-in-one). Adapted with permission.[2] Elsevier, 2015; (b) Microvascular self-healing is built in by a finely designed vascular network, including one-dimensional (1D) networks made from hollow channels/fibres filled with healing agents, 2D and 3D vascular healing networks require cultivated manufacturing to guarantee connectivity. Adapted with permission.[4] Elsevier, 2017.

In contrast, intrinsic self-healing processes are performed through the use of reversible dynamic covalent bonds or supramolecular interactions within the polymer structure, which have the capacity to interact and reform the microstructures under specific conditions, so that they perform multiple healing cycles autonomously.[5] As shown in Figure 3A~~a~~, intrinsic self-healing of polymers can be achieved by dynamic covalent bonds via associative or dissociative exchange reactions,[6] such as disulfide metathesis, imine transamination, radical-based exchange systems, or reversible Diels-Alder reactions. Supramolecular interactions include hydrogen or halogen bonds, ionic interactions, π–interactions, host–guest interactions, metal–ligand interactions and hydrophobic interactions.[7] In addition, through surface functionalisation of nanoparticles, exchangeable reactions can also occur at the interfaces of nanoparticles and polymer matrices to assist in self-healing at interfaces. The detailed introduction of the dynamic reactions for covalent polymer networks for self-healing and reprocessable polymers can be found from recent detailed reviews,[5, 8, 9] along with the latest applications of self-healing polymers in smart devices.[10, 11]

The ability of a polymer to intrinsically self-heal depends on its chain mobility and the exchange kinetics of its dynamic bonds. When the two new surfaces make contact with each other, dynamic bonds exchange and the mobility of the polymer chains allows for structural reformation to recover properties. However, to heal damage such as a mechanical crack, there is generally a need for an intimate contact between the separated surfaces to allow the polymer

chains to interact, diffuse or react. The introduction of *shape-memory* properties by tuning the phase morphology or crystalline domains can allow shape recovery and enable fractured surfaces to re-connect with each other, thereby assisting in the healing process.[12] The efficiency of the self-healing process depends on the nature of the reversible bonds and the healing conditions, which can be enhanced by a combination of multiple healing mechanisms, such as shape-memory assisted self-healing (Figure 3B~~b~~), soft-hard microphase separation (Figure 3C~~c~~) or using nanocomposites (Figure 3D~~d~~). Now that the range of healing mechanisms have been introduced, the range of potential hostile environments that self-healing may be needed is described.

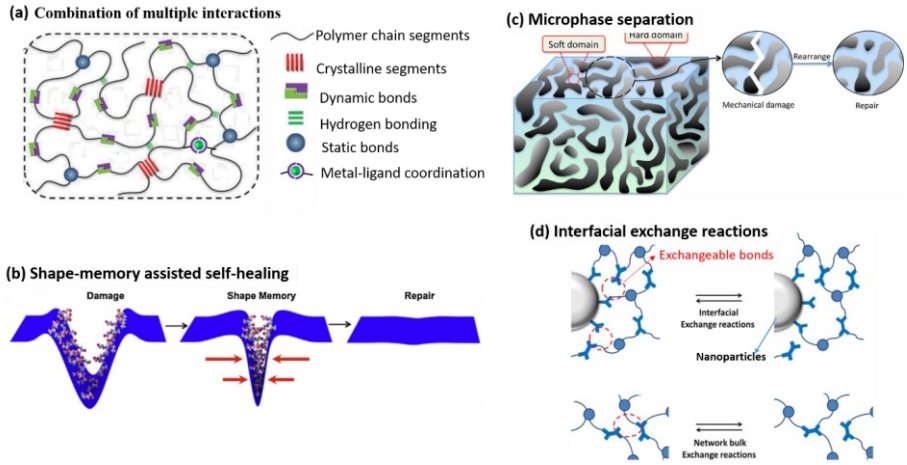

Figure 3 Strategies for creating intrinsic self-healing polymers, including dynamic covalent and non-covalent bonding: (a) The combination of multiple interactions. Adapted with permission.[13] John Wiley and Sons, 2020. (b) Shape-memory assisted self-healing. Adapted with permission.[14] Elsevier, 2015. (c) Soft-hard microphase separation. Adapted with permission.[14] Elsevier, 2015. (d) Interfacial exchange reactions (vitrimer chemistry) via surface functionalised nanoparticles. Adapted with permission.[15] American Chemical Society, 2016. ~~These are promising approaches to enhance the self-healing efficiency and tailor the healing timescale.~~

3. Self-healing under extreme environments

In this section a range of self-healing processes which operate in extreme environments will be overviewed. This will include operation at high or low temperature, or subject to high cycle fatigue, underwater, corrosive, vacuum and high intensity UV, electric or magnetic field environments. The self-healing performance of different systems are compared in Table 1.

3.1 Self-healing at high temperatures (> 100°C)

For intrinsically self-healing materials, reversible Diels-Alder (DA) cycloadditions are a commonly employed mechanism due to their inherent simplicity, reversibility and repeatability.[16] Reactions between furan and maleimide,[17] or anthracene and maleimide,[18] have been used for self-healing, where the thermal reversibility of the reaction imposes limitations on its application areas. The retro-DA reaction of furan-maleimide adducts occurs at approximately 120 °C, and therefore above this temperature the mechanical properties of these materials decline due to a reduction in the number of crosslinks. Anthracene-maleimide adducts are cleaved at higher temperatures, up to 250 °C, which is often beyond the decomposition temperature of the polymers.[19] This has been overcome by using anthracene and maleimide moieties to achieve high temperature self-healing in carbon fibre reinforced polymers composites (CFRP) at 250~300 °C.[16]

As shown in Figure 4~~(~~A~~a)~~, 9-anthracenemethanol and N-(2-hydroxethyl)-maleimide were cross-linked prior to their reaction with hexamethylene diisocyanate (HDI) to synthesise a viscous liquid premonomer (HDTA), which eliminated~~-the~~ the need for a ~~need for~~ solvent ~~needss~~ or melting ~~requirements for~~ ~~in the~~to processing ~~of~~ bulk specimens. P~~The p~~olyurethanes with a higher molar ratio of HDTA/HDI exhibited improved self-healing properties, as healing requires crack propagation to form~~occur~~ predominantly~~imarily~~ through the Diels-Alder bonds. The healing efficiencies were 94%, 78% and 77% for the first, second and third healing cycles, respectively. The polymer exhibited a high physical and mechanical stability at temperatures

Formatted: Font color: Dark Red

up to 240 °C. Furthermore, the fabricated CFRP composites containing ~~the~~ self-healing polyurethane and unidirectional carbon fabrics produced healing efficiencies of 69.1% and 52.4% for the first and second healing cycles, respectively. The lower self-healing efficiency of the composites was attributed to failure of the fibres, ~~as~~ the main~~primary~~ load-~~-~~bearing components~~s~~, and delamination at the interface between reinforcing fibres and the polymer matrix. Overall, the work demonstrated the use of Diels-Alder chemistry for prolonged high temperature healing using a solvent-free polymerization method. Shape memory polymers can be also incorporated as a strategy to bring the cracked faces into contact, as in Figure 3~~3~~B~~b~~, and remove the requirement for human intervention to initiate self-healing.

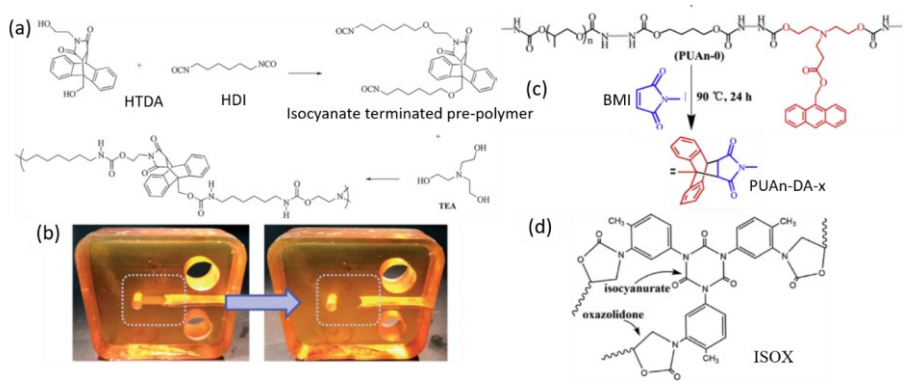

Figure 4 (a) Polymerization of HTDA, TEA, and HDI monomers; (b) one 0.8HTDA1T specimen showing before (left) and after healing (right), where 0.8HTDA1T was synthesized with 0.8 moles of DA polymer HTDA, 1 mole of TEA and 2.3 moles of HDI. A greater molar fraction of the healable HTDA molecule promotes healing. Reproduced with permission.[16] Royal Society of Chemistry, 2016. (c) Linear polyurethane (PUAn-0) bearing pendant anthryl chromophores and BMI induced cross-linked PUAn- Diels-Alder –x. Adapted with permission.[20] Elsevier, 2018. (d) Chemical structure of isocyanurate-oxazolidone (ISOX) thermosets. Reproduced with permission.[21] Elsevier, 2018.

Recently, a series of thermostable self-healing linear polyurethane elastomers have been reported, which use retro-Diels-Alder reactions initiated by thermal and mechanical stimuli

between anthryl and maleimide groups.[20] The polyurethanes bore pendant anthryl groups which covalently cross-linked with bismaleimide cross-linkers, as shown in Figure 4(c). To evaluate the healing process, the cross-linked specimens were cut and kept at 90 °C. The polyurethane chains and hydrogen bonds rearranged as~~with~~ the ~~expansion of the~~ crack surfaces expanded during heating and the heat treatment led to the recombination of the Diels-Alder bonds, which reformed~~generated~~ the ~~structure of the~~ network ~~structure~~ structure and regenerated~~stored~~ its mechanical properties. The healing efficiency reached a maximum of 91% with respect to ultimate tensile strength for the polyurethane with a 1:1 ratio of anthryl to maleimide functional groups, respectively. With regards to the thermal stability, decomposition was observed above 250 °C, which was ascribed to the decomposition of the urethane bonds.

An intrinsically healable isocyanurate-oxazolidone (ISOX) thermosetting matrix was applied to CFRP composites, as shown in Figure 4(d).[21] The ISOX polymer utilized commercial diglycidyl ether of bisphenol F and toluene diisocyanate to produce a high cross-link density thermoset with a T_g of up to 285 °C. The high T_g was derived from the bulky ring structure of the isocyanurate and oxazolidone primary components, along with the high cross-link density. The ISOX resin/carbon fabric composites showed the highest healing efficiency of 85% for a composite containing the highest amount of toluene diisocyanate. This was ascribed to molecular chain scission of the isocyanurate under mechanical stress and the transformation of the isocyanurate with epoxide groups to yield new oxazolidone rings at the fracture surface.[22] With regards to thermal stability, the composites began to decompose at ~350 °C in both air and nitrogen and more than 99.5% of the composite weight remained when the temperature reached 300 °C. The employed healing mechanism proved to have a more substantial effect on the self-healing of the CFRP composite than that of Diels-Alder chemistry.

Formatted: Font color: Dark Red

Formatted: Font color: Dark Red

Formatted: Font color: Dark Red

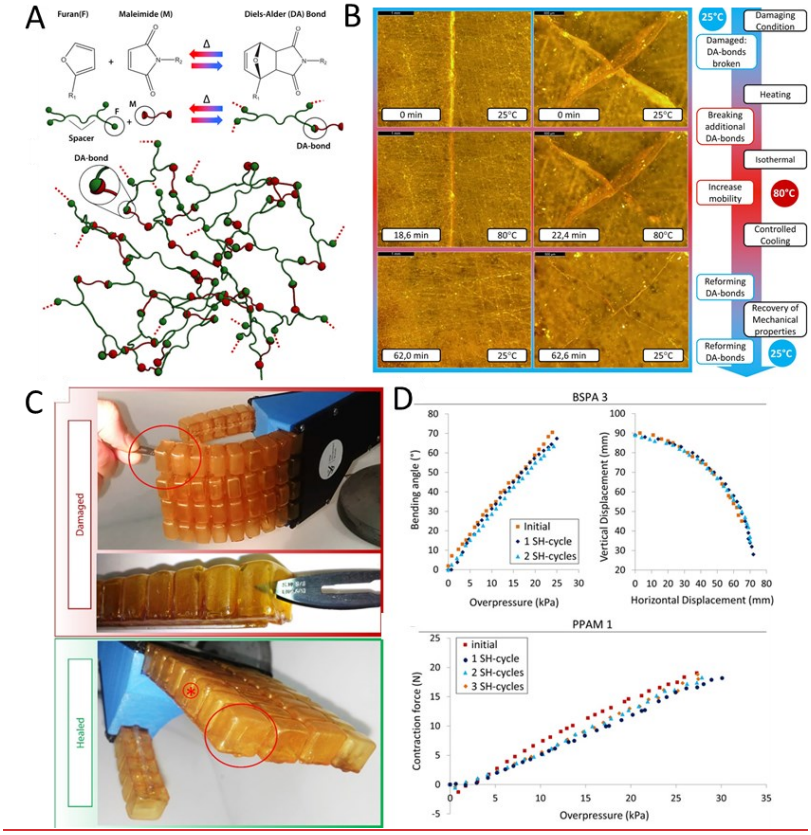

Figure 5. Diels-Alder based soft self-healable pneumatic actuators and robotic hand under a high temperature environment. (A) Diels-Alder cross-links and its thermo-reversible network. (B) Self-healing process of Diels-Alder polymers used for manufacturing pneumatic actuators. (C) Demonstration of the damaged and healed Diels-Alder-based robotic hand. (D) Bending angle, vertical displacement and the contraction force of the undamaged and healed robotic hand. Reproduced with permission.[23] The American Association for the Advancement of Science, 2017.

A range of intrinsic self-healing devices have been fabricated for high temperature applications. Terryn *et al*. designed a self-healing soft pneumatic actuator using Diels-Alder chemistry, as shown in Figure 5A.[24] Two damage conditions were considered, (i) a small perforation when

the actuator was over pressurised at 0.46 bar and (ii) a deep wall cut of a length of 4.43 mm and a thickness of 0.3 mm. Both forms of damage were successfully healed after 30 hours at a maximum temperature of 70 °C. ~~Figure 5(C) shows the steady state force before and after self-healing process and the soft pneumatic cell was fully cured.~~ The group also demonstrated three self-healing applications using the self-healing Diels-Alder polymers, including a soft gripper, a soft hand, and artificial muscles. The devices self-healed after a heat treatment of 80 °C for 40 min before~~and~~ gradually~~slowly~~ cooling to 25 °C. After 24 hours at 25 °C, the initial properties were almost completely~~entirely~~ recovered.[23, 25] The group has also successfully manufactured a sacrificial self-healing mechanical fuse using Diels-Alder chemistry, as shown in Figure 5C~~D and Figure 6~~, which was validated on a cable-driven robotic system which could self-heal at a temperature of 120 °C for 170 min.[26]

Formatted: Font color: Dark Red

Formatted: Font color: Dark Red

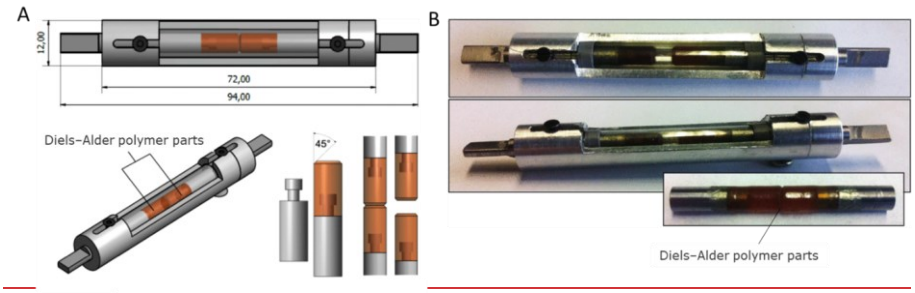

~~Figure 6 (a) self-healing mechanical fuse design and (b) manufactured prototype. Reproduced from Terryn *et al.*~~

Formatted: Normal, Justified

The ability to change the shape of a 3D printed object as a function of time is known as *4D printing*.[27] The shape-changing behaviour of shape memory polymers is attracting researchers in the search for materials to create new actuators for soft robotics, along with potential applications in 4D printing. Invernizzi *et al*.[27] developed 4D-printed thermally activated self-healing and shape memory polycaprolactone-based polymers, which has been used to print an

actuator, as shown in Figure 67. The shape memory functionalities were preserved after healing under 80 °C.

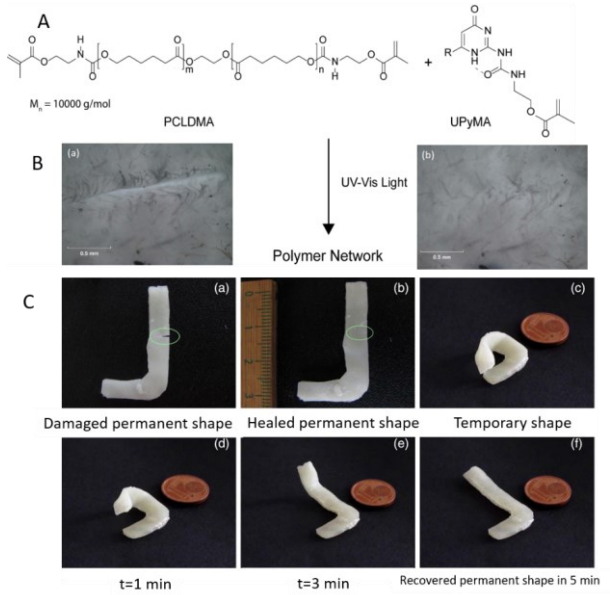

Figure 67 4D printed thermally activated self-healing and shape memory polycaprolactone-based polymers. (A) Chemical scheme of the crosslinking reaction between polycaprolactone dimethacrylate (PCLDMA) and (2-ureido-4[1H]-pyrimidinone motifs) UPyMA. (B) Self-healing process for PCLDMA-UPyMA printed samples. Images of the superficial cut pre- (a) and post- (b) thermal treatment at 80 °C. (C). Shape memory effect of PCLDMA-UPyMA repaired samples. Specimen was cut (a) and thermally treated for 1 h at 80 °C (b). The deformed object (c) was heated at 70 °C to enable full recuperation of its original shape (d–f). Reproduced with permission.[27] Elsevier, 2018.

A photopolymerization-based additive manufacturing technique to form self-healable elastomer structures with free-form architectures has been developed.[28] The process depends on a molecularly designed photo-elastomer ink with both thiol and disulfide groups. The thiol groups facilitate thiol-ene photopolymerization reactions during the additive manufacturing process and the disulfide groups enable disulfide metathesis reactions during the self-healing

process. 3D soft actuators were manufactured using rapid additive manufacturing of single- and multi-material self-healable structures, as shown in Figure 7~~8~~. The actuators were healed at 60 °C for 2 hours, and the mechanical properties were fully recovered. The results show the photo-elastomer can be an effective solution for fabricating self-healing free-form architectures. Vanderborght *et al*. used additive manufacturing method to fabricate thermo-reversible Diels-Alder polymers, which has been successfully demonstrated on a soft robotic gripper.[10] The gripper can be 95% recovered from large cuts, tears, and punctures, after healing for 30 min at 90 °C, which can be used for high-temperature environments.

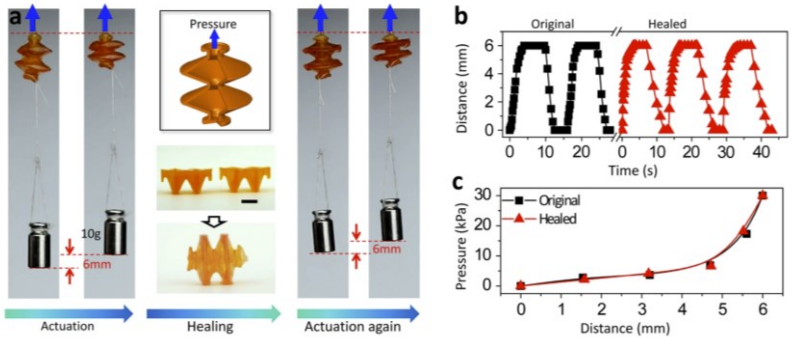

Figure 7~~8~~ Self-healable 3D soft actuator. (a) Negative pressure actuation enabled the additively manufactured elastomer actuator to lift the 10 g weight by 6 mm. The inset shows the elastomer actuator CAD model. The actuator was severed and recontacted to heal for 2 h at 60 °C. The self-healed actuator can be reactuated by the negative pressure to lift the 10 g weight by 6 mm. The scale bar represents 5 mm. (b) The cyclic lifting distance of the 10 g weight as a function of time of the actuators before and after healing. (c) The trend between the negative pressure values versus lifting distance of the actuators, before and after healing. Reproduced with permission.[28] Springer Nature, 2019.

In addition to developing polymer matrices with intrinsic self-healing properties, extrinsic approaches are also used to achieve high temperature healing. For example, a trifluoromethanesulfonic acid (TfOH), a strong Brønsted acid, was encapsulated in silica

microspheres and mixed with an epoxy monomer to form a self-healing agent.[29] The self-healing epoxy that contains both epoxy- and TfOH-loaded capsules did not undergo decomposition at temperatures below 300 °C, although for the TfOH-loaded capsules a weight change was observed due to the volatilization of TfOH. The matrix epoxy obstructed the escape channels of the volatile TfOH and the composite was therefore able to withstand high temperature exposure. Cationic chain polymerization formed the basis of the curing mechanism of the epoxy when catalysed by the strong Brønsted acid. A self-healing system based on a 10 wt% epoxy loaded-microcapsules and 0.6 wt% TfOH loaded-microcapsules exhibited a maximum healing efficiency of 79% after 100 seconds with respect to impact strength. This level of healing efficiency was possible even after 10 months of open-air storage, indicating there was no surface ageing, and that TfOH did not exert a noticeable negative impact on the healed epoxy. Therefore, the healing system was stable for long-term storage at room temperature and also thermally stable within a high temperature environment. However, since the microcapsules can only release a limited amount of healing agent, the system is best suited for the elimination of only small scale micro-cracks. It was noted that the balance between the rate of curing and the speed of healing agent delivery would require further consideration for larger scale damage sites; there is potential to examine the use of a microvascular network (Figure 3B) using this healing chemistry.

3.2 Self-healing at low temperatures (< 0 °C)

Polymer chain mobility is important to the self-healing process and enabling the recovery of properties after damage. At temperatures below the glass transition temperature, T_g, of a polymer, the chains have restricted mobility, thereby making it more challenging for polymers to self-heal. For example, the trans-Siberian railway, reaching from Moscow to Vladivostok (over 9000 km), frequently experiences temperatures lower than -20 °C and in aerospace

applications, aircraft parts can be exposed to temperatures as low as -60 °C.[30] It is also critical that self-healing materials can function in extreme environments with temperature fluctuations between -150 and 150 °C. This has led to high demands on the performance of self-healing material, which require (i) chemical stability and high thermal stability of the self-healing components (catalysts and vessels filled with healing agents) and (ii) high healing efficiencies at low temperature.[31]

Extrinsic healing methods are often applied for low-temperature self-healing, via the use of microcapsules, hollow vessels and conductive heating elements.[2, 32] Alternatively, low-temperature intrinsic self-healing methods have included hydrogen bonding, azide/alkyne click reactions and metal-ligand interactions.[33-35] This section will discuss the progress made in these areas coupled with their apparent limitations.

Extrinsically self-healing materials often employ liquid resins or solvents that are microencapsulated within the matrix. The curable resin is released into the damaged area and subsequent polymerization of the resin is triggered by an embedded catalyst, thereby healing the damaged area.[36] This method has been adapted to produce materials that can ~~arecan~~ self-heal~~able~~ in ~~at~~ low-temperature environments. For instance, microencapsulated diglycidyl ether of bisphenol A and diglycidyl tetrahydro-o-phthalate epoxy resins, with mercaptan as a hardener, were used as a two-component healing agent embedded in an epoxy matrix, with benzyl dimethylamine as the healing catalyst.[37] The microcapsules were able to interface with the matrix via hydrogen bonding through polar amine and hydroxyl groups on their melamine-formaldehyde shells. This interaction promoted crack penetration~~the penetration of cracks~~ through the encapsulated healing agent during mechanical damage. In terms of recovery of fracture toughness, the healing efficiencies was greater than 82% at 20 ºC after 3 hours and over 100% after 12 hours. The self-healing process slowed ~~down~~ with decreasing temperature, but continued to exhibit an 86% recovery at -10 ºC after 36 hours. These indicated that high

Formatted: Font color: Dark Red

Formatted: Font color: Dark Red

healing ~~efficiencies~~ are ~~can~~ obtainable~~be acquired~~ at low capsule contents (2.5 wt% epoxy-loaded capsules and 2.5 wt% hardener-loaded capsules). This characteristic, when~~,~~ coupled with the ~~benefit~~ fact that epoxies have a high~~greatood~~ adhesion to a ~~good spread~~wide variety ~~of~~~~many~~ materials, mak~~es~~~~ing~~ it an ideal candidate as a versatile healing agent. However, it was observed that the temperature of -10 ºC is the lower limit, which is not sufficiently low for colder applications, such as aerospace. It should be noted that the self-healing performance of the system was evaluated at room temperature, which can enhance fluid transport throughout the damaged region, yielding artificially high values of healing efficiency. Another similar example is the study of the polymerization of a 5-ethlidene-2-norbornene/dicyclopentadiene healing agent at -50 ºC for aerospace applications,[38] where a healing efficiency of 72% was reported. Thus, the complete thermal history of the system should be considered when interpreting self-healing performance.

The low-temperature self-healing behaviour of a microcapsule-type protective coating has also been demonstrated.[30] A silanol-terminated polydimethylsiloxane (STP) and a dibutyltin dilaurate catalyst were encapsulated by urea-formaldehyde polymer and polyurethane as the shell materials, respectively. ~~After mixing~~ T~~t~~he microcapsules were mixed into a commercial enamel paint~~,~~ and~~when the paint was~~ subjected to scratching at a temperature of -20 °C. T~~the healing agents were readily released from the~~ his ruptured the microcapsules and released the healing agests, which~~to~~ filled and healed the damaged regions. The condensation reaction of STP silanol end-groups were responsible for the curing process and reached 83% conversions at -20 ºC after 19 days. The low-temperature self-healing was evaluated by corrosion, electrochemical and saline solution permeability tests and produced positive results, demonstrating the applicability of the system, particularly for cementitious applications in cold environments. However, it was assumed that the percentage conversion of silanol end-groups translated into similar mechanical and/or electrochemical recoveries, and requires further study.

Formatted: Font color: Dark Red

Formatted: Font color: Dark Red

Formatted: Font color: Dark Red

Formatted: Font color: Dark Red

Formatted: Font color: Dark Red

To operate at even lower temperatures using extrinsic self-healing (< -20 °C), Wang *et al.* proposed an approach using two components based on a three-dimensional vessel and a thin layer of conductive material.[32] The design involved embedding the two components into a glass fibre-reinforced laminate composite with vessels to deliver and release the healing agents, with a thin conductive layer to supply heat by Joule heating and provide a suitable temperature for healing; this is shown Figure 8~~9~~. The conductive layer was fabricated from either a porous copper foam sheet or porous carbon nanotube sheet. For the system containing carbon nanotube sheets, an applied voltage between 10 and 16 V achieved a steady-state temperature in the range of 20 to 85 °C, which de-iced the composite in 90 s and enabled curing within 24 hours to achieve healing. After 24 hours of healing at -60 °C, the composite with carbon nanotube sheets exhibited average healing efficiencies of approximately 107% and 96% with respect to fracture energy and peak load respectively. An ~~Only a small~~ electrical current of only 200 mA was required to generate the heat, reducing the probability of severe thermal hotspots that could lead to damage. This vessel-based design was advantageous compared to capsule-based designs as healing agents could be continuously pumped into the vessels and the vessel network had only a minor effect on the tensile strength. This provides a novel solution to solve the problem of effective low-temperature self-healing for applications such as in-flight aircraft and satellites, as well as offshore appliances such as wind turbines. This approach also overcomes the problem of a narrow active temperature range for the healing agents employed.

Formatted: Font color: Dark Red

Formatted: Font color: Dark Red

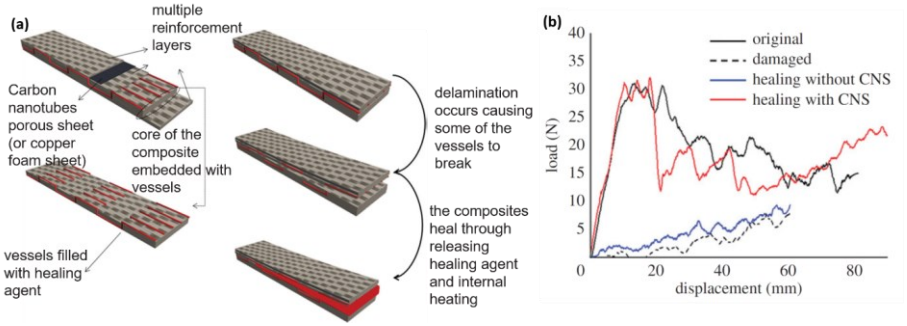

Figure 8~~9~~ (a) Laminate composite structure and the damage-bleeding-healing self-healing process; (b) displacement–load curve for a typical sample incorporating porous carbon nanotube sheets (CNS), Reproduced with permission.[32] Royal Society, 2016.

Formatted: Font: Not Italic

An intrinsically self-healing matrix that utilizes associative or dissociative chemical bonds has the ability to break and reform when damage occurs; the chemical bonds can include reversible dynamic covalent bonds or non-covalent interactions. The combination of different dynamic bonds provides opportunities to expand the self-healing thermodynamics and kinetics by the selection of the dynamic bonds. For example, Kalista *et al*. took advantage of hydrogen bonding and ionic association interactions to produce a specific class of poly(ethylene-co-methacrylic acid) (EMAA) copolymers and ionomers with the ability to autonomously self-heal ballistic projectile punctures at low-temperature within a wide operational temperature range.[39] A range of EMAA copolymers varying from non-ionic to highly neutralized were studied to explore the relationship between ionic content, morphology and the self-healing response to ballistic impact. The mobility and strength of the associated regions of the non-neutralized non-ionic copolymers and of the ionomers with partially neutralized methacrylic acid groups arose from the introduction of hydrogen bonding and ionic association interactions respectively. During ballistic puncture testing, the energy was transferred to the punctured film and could be stored elastically to facilitate closure of the hole; energy can also be lost via

heating or permanent viscous deformation. Localized heating is critical to the healing mechanism, allowing material softening to produce scars followingthe scar upon elastic closure and subsequent welding of the puncture sites. The ballistic puncture test revealed that an ionomer with 30% of the methacrylic acid groups neutralized produced the greatest degree of self-healing in the temperature range from -50 °C to 110 °C. Purely non-ionic non-neutralized copolymers demonstrated a brittle behaviour at temperatures below 10 °C. Ionomers with 60% neutralization were highly ionic and this led to a decrease in the self-healing ability since an increase of ionic domains led to a more densely packed system, thereby leading to a decrease in chain mobility. A moderate ionic content improved the self-healing properties by providing both strength and chain mobility at low temperatures. This work both demonstrated healing over a wide temperature range with a low-temperature limit and rapid healing. This makes the material attractive for use applications such as combat aircraft fuel tanks or as a resilient protective barrier of protection in oil tankers or other containment applications.

Formatted: Font color: Dark Red

Formatted: Font color: Dark Red

Formatted: Font color: Dark Red

Similarly, Yang *et al.* designed a conductive organo-hydrogel with antifreeze self-healing ability through the use of hydrogen bonding and electrostatic interactions.[35] A series of gels were prepared by radical polymerization under a water-glycerol mixed solution with sodium methacrylate (MAANa) and [2-(methacryloyloxy)-ethyl] trimethyl ammonium chloride (DMC) as monomers. Usually, the water segment of conductive hydrogels freezes at low temperatures. However, the addition of glycerol to the hydrogel reduced the freezing point to -46.5 °C, although it could inhibit the ionization of the polyelectrolyte and decrease the self-healing ability. The gels exhibited electrically conductive properties based on the presence of ionic polymer networks., Thiswhich released a large greatlarge amountnumber of free-moving ions by ionization of water, thereby achievingproviding a degree ofgranting electrical conductivity. The self-healing efficiency was 96% (20 °C), 94% (4 °C) and 85% (-20 °C), respectively, after only 5 seconds of healing when damaged surfaces were in close contact

(Figure 9A~~C~~). In addition, the high stretchability (~7000%), non-toxicity of glycerol and the ability to adhere to skin provides potential to use this material in motion sensing wearable devices and signal transition materials, where it would be particularly effective for use in extremely cold regions.

Hydrogen bonding, coupled with ionic or electrostatic interactions, have proven to be effective for extreme low temperature healing. In addition, metal-ligand interactions are also effective in low-temperature self-healing materials. For example, a network of poly(dimethylsiloxane) polymer chains cross-linked by three different interactions: a strong pyridyl–iron interaction, and two weaker carboxamido–iron interactions through both the nitrogen and oxygen atoms of the carboxamide groups.[34] The iron-ligand bonds ~~readily~~ easily break and re-form, whilst the iron centres remain boundattached to the ligands through ~~the~~ stronger interactions with the pyridyl ring, enabling reversible ~~un~~folding and un~~re~~folding of the chains, as shown in Figure 9A~~B10~~. This enabled the material to heal at temperatures as low as -20 °C with a healing efficiency of 68% for the fracture strain after a period 72 hours where the two severed pieces were in close contact. The maximum fracture strain reached up to 4500% due to the metal-ligand intrachain and interchain interactions. In addition, surface ageing and moisture did not significantly affect the material, as is often seen with hydrogen bonding.[40] These features, coupled with the fact that the material has a high dielectric constant ($\varepsilon_r \sim 6.4$) and dielectric strength (18.8 MV m^{-1}), make it extremely suitable for application towards self-healing artificial muscle actuators.

Formatted: Font color: Dark Red

Formatted: Font color: Dark Red

Formatted: Font color: Dark Red

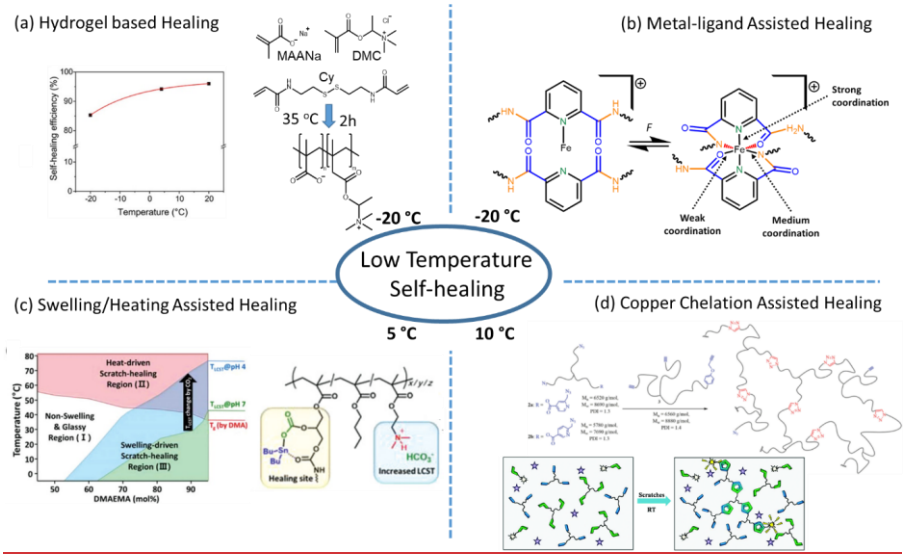

Figure 9~~10~~ (a) Self-healing efficiency of conductive hydrogel at different temperatures. Adapted with permission.[35] American Chemical Society, 2019. (b) Fe(III) ion-2,6-pyridinedicarboxamide coordinated $[Fe(Hpdca)_2]^+$ moiety undergoing reversible breakdown and reformation.[34] (c) Diagram showing relationship between self-healing temperature and 2-(dimethylamino) ethyl methacrylate (DMAEMA) content of a switchable self-healing random copolymer in the presence of CO_2 and H_2O: I-region where there is no self-healing; II and III-regions whereby heat and swelling mediate self-healing, respectively. Reproduced with permission.[41] John Wiley and Sons, 2018. (d) Network formation of star-shaped azido-telechelic PIBs (2a or 2b) and PIB-alkyne (3) utilizing chelation-assisted CuAAC to self-heal fast at 10 °C. Reproduced with permission.[33] Royal Society of Chemistry, 2016.

Similarly, random copolymers were prepared from 2-(dimethylamino)ethyl methacrylate (DMAEMA), glyceryl monomethacrylate (GlyMA), and butyl methacrylate monomers via free-radical polymerization.[41] The GlyMA units form metal–ligand coordination complexes with dibutyltin dilaurate, leading ~~to~~to the formation of ~~the formation of~~ new carbonate bonds ~~formations~~ under ambient CO_2 and H_2O conditions. The copolymers could be healed below their T_g by combining metal–ligand coordination and the modulated lower critical solution

Formatted: Not Highlight

Formatted: Font color: Dark Red

Formatted: Font color: Dark Red

temperature (LCST). Swelling at temperatures below the LCST was necessary to promote ~~the interdiffusion of~~ polymer chain interdiffusions ~~and~~to ~~enable~~accomplish self-healing, but this led to a decrease~~reduction in~~ed mechanical strength. Furthermore, increasing the DMAEMA content increased the degree of self-healing, but ~~also led to at the~~was also detriment~~als~~ to the mechanical strength. As a result, optimization of DMAEMA content was necessary to achieve the appropriate balance of healing and strength, as shown in Figure 9C~~D~~. The greatest degree of self-healing was observed at *pH* ~ 4 at a temperature of 5 ºC for a DMAEMA content of 60%. The material recovered almost 100% of its mechanical properties after wetting for 1 hour and drying for 3 hours. In addition, the material was able to recover its mechanical properties after ten cycles of wetting and drying. These properties make the material suitable as a coating for materials in cold or acidic environments.

However, the mechanical properties are only recovered in the drying stages and are lost during the wetting/swelling stage.

Whilst a temperature 5 ºC cannot be fully ~~described~~ considered as ~~being~~ extreme, it is worth highlighting the approach used to lower the healing temperature to below room temperature. It would be of interest in future efforts to exploit the method through optimization or conjoining with other techniques to more extreme low temperatures. In addition, the healing of copolymers below their T_g is an intriguing concept which could be of greater significance in future research, and healing in more acidic conditions is a theme explored later within this review.

In addition to hydrogen bonding and metal-ligand interactions, Deng *et al.* synthesized intrinsically self-healing impact hardening polymers which utilized reversible dynamic cross-linking of boron compounds to impart self-healing.[42] The impact hardening polymers were synthesized by condensation copolymerization of silicone polymers with various chain lengths and boron contents and had a maximum healing efficiency of 89% at room temperature for 18 hours. The material could also self-heal at temperatures as low as -25 °C with efficiencies

Formatted: Font color: Dark Red

Formatted: Font color: Dark Red

Formatted: Font color: Dark Red

above 80% when healed for 30 hours. Increases in the polymeric chain length of the backbone reduced the threshold entanglement density. This, coupled with the reversible dynamic cross-linking boron junctions, enabled healing at low temperature as well as achieving high energy absorbing properties, and improving the fatigue resistance of the material overall. Alternatively, Neumann *et al.* reported a self-healing system containing star-shaped picolinazido- and alkyne-telechelic polymers based on poly(isobutylene), forming a network with the aid of chelation-assisted copper catalysed azide/alkyne 'click' reactions, as shown in Figure 9D~~B~~.[33] A complete cross-linking of the components was observed within 71 minutes at 10 °C, achieving fast healing below room temperature using 'click' reactions.

3.3 Self-healing of cyclic fatigue damage

Safety is a major concern for structurally integrated systems such as aircraft, jet engines and power plants. During operation, complex structures experience a variety of forms of alternating stresses, or are subjected to demanding environments where time dependent degradation processes occur, such as creep and fatigue. When a material or structure is subjected to loading/unloading cycles, the fatigue process can initiate progressive and localised structural damage, such as crazes, microcracks or delamination. The damage can continuously grow until defects reach a critical size that ultimately leads to final fracture.

Structural polymeric composites are subjected to fatigue loading in their service lifetime. One example is the adhesive failure at the interfaces of different components of composites, whereby the adhesive loses its adhesion to one of the bonding surfaces as a result of the hydration of the chemical bonds which form the connection between the adhesive and the bonding surface[43], as shown in Figure 10~~A~~a. This can be mitigated with surface preparation techniques, while adhesive debonding can be difficult to detect using non-destructive techniques. A different mode of failure, cohesive failure, can also be taken into consideration. Cohesive failure is the breakdown of intermolecular bonding forces, occurring primarily in the

bulk layer of an adhesive substance,[43] see Figure 10~~1~~B~~b~~, or combined adhesion and cohesion failure (Figure 10~~1~~C~~c~~). Other crack growth mechanisms include matrix cracking and fiber/matrix debonding which mainly affect fibre-reinforced polymer (FRP) composites, as seen in Figure 10~~1~~D~~d~~. FRP laminated composites frequently undergo delamination as a failure mode, resulting from cyclic fatigue loading or low velocity impact events.[44] In order to mitigate the aforementioned events of polymeric structural materials, researchers have sought to incorporate self-healing mechanisms as a means to retard crack growth and extend the service lives of the materials. This section will discuss the progress made in this area coupled with their apparent limitations.

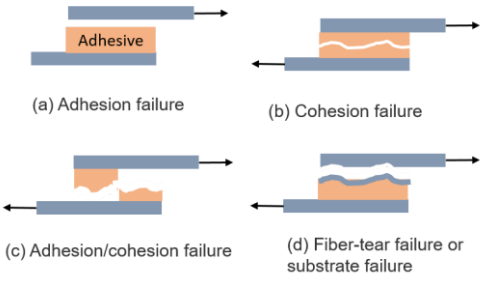

Figure 10 ~~1~~Illustration of common failure mode types for adhesive joint systems. (a) interfacial failure separation between adhesive and adherend surface, (b) cohesive failure separation within the adhesive, (c) adhesion/cohesion failure; (d) fiber-tear failure separation within the fiber-reinforced plastic, or substrate failure.

Microcapsules act as an extrinsic means to introduce self-healing functionalities into polymeric materials to prevent and heal fatigue damage. White *et al*. pioneered this method of healing in 2001 with the first structural polymeric material capable of healing autonomously, utilizing a living ring-opening metathesis polymerization and invoking the use of a transition metal catalyst (Grubbs' catalyst).[36] In self-healing elastomers, the propagation of fatigue cracks due to fatigue loading is retarded by a range of mechanisms, such as hydrodynamic crack tip

shielding, adhesive bonding and artificial crack closure.[45] An additional mechanism for torsional fatigue relates to theis based on frictional contact between crack faces, that are induced and accentuated by the healed polymer delivered uponto the crack plane. Following this principle, Keller *et al.* synthesized a self-healing material which consisted of a microencapsulated vinyl-terminated poly(dimethylsiloxane) (PDMS) resin containing platinum catalyst and a microencapsulated initiator (methylhydrosiloxane).[46] There was Sprofoundsignificant surface abrasions were present on the crack faces of the specimens containing the active healing chemistry, which. These abrasions and were associated with an operative *sliding-crack-closure* mechanism., Thiswhich reduced the effective stress at the crack front and led to a noticeable observed reductions of the terminal crack length in the torsion fatigue specimens. A second mechanism was proposed where the healing agent polymerizes and interacts with surface asperities on the crack faces to escalatefacilitateintensify the closure mechanism, thereby producing sharp increases in torsional stiffness. The generation of new polymers with the aforementioned shielding mechanisms reduced the apparent crack tip loading to slow crack propagation and the authors reported a 24% reduction in total fatigue crack growth after 5 hours of curing.[46]

Furthermore, self-healing epoxies undergo similar shielding mechanisms. Epoxy resins strongly adhere to most inorganic surfaces typically due to strong polar attractions to oxide or hydroxyl surfaces. An extrinsically self-healing epoxy adhesive was reported for bonding steel substrates, using encapsulated dicyclopentadiene (DCPD) monomer and Grubbs' catalyst particles dispersed in a thin epoxy matrix.[47] The steel bonding surfaces was subject to mechanical abrasion, cleaning, and the application of a silane agent coupling was applied to promote cohesive failure through the self-healing adhesive. The incorporation of incorporation of microcapsules and catalyst particles into the adhesive corporation promoted crack path deflection from the substrate/adhesive interface into the adhesive layer for the self-healing.

Formatted: Font color: Dark Red

Formatted: Font color: Dark Red

Formatted: Font color: Dark Red

Formatted: Font color: Dark Red

Formatted: Font color: Dark Red

Formatted: Font color: Dark Red

With these additions, the virgin fracture toughness increased by 26%, and self-healing specimens recovered 56% of their virgin fracture toughness after 24 hours of healing at room temperature. Furthermore, the self-healing samples exhibited complete crack arrest after 150,000 cycles, compared to that of the pure resin that failed at less than 62,000 cycles. This work demonstrates an increase in the lifetime of the material using self-healing to mitigate against progressive fatigue damage.

Similarly, Kim *et al*. designed a self-healing laminated composite with embedded microcapsules that was fabricated from unidirectional glass/epoxy prepreg.[48] The microcapsules contained a mixture of ethyl phenylacetate (EPA) solvent and diglycidyl ether of bisphenol A (DGEBA) epoxy and were incorporated into cross-ply laminated composites. The microcapsules increased the resistance to ~~the resistance to crack growth~~crack growth ~~resistance~~ due to ~~the~~ shear yielding of the matrix near the cavities, and the release of EPA locally acted to plasticize the matrix that eventually delayed the ~~saturation of~~ saturation of transverse cracks~~ saturations~~. The self-healing specimens were allowed a 24-hour rest period at ambient conditions, following tension-tension fatigue testing ~~in order~~ to ~~enable~~ allow the crack faces to rebond, requiring additional fatigue cycles to reopen these cracks. A healing efficiency of 52% was reported for the self-healing composite with respect to its initial Young's modulus. The number of fatigue cycles at the saturation of transverse cracks was 2.7 times higher for the self-healing composites (~10,550 cycles) compared to the control composites (~3,800), ~~showing~~ demonstrating an increase in crack growth resistance.

Intrinsic self-healing methods have also been investigated to combat fatigue damage. Kostopoulos *et al.* investigated the self-healing functionality of a bismaleimide self-healing resin, based on a Diels-Alder reaction mechanism, which was integrated into high performance aerospace carbon fibre reinforced plastics (CFRPs).[44] A prepolymer from DGEBA with furfuryl amine was synthesised and reacted with BMI, the reversible Diels-Alde crosslinker,

Formatted: Font color: Dark Red

prior to integration within the CFRPs. The authors conducted fFatigue tests ~~were performed~~ following three different routes: continuous loading, fatigue loading with "interruptions" every 10,000 cycles and fatigue loading with "interruptions" together with healing cycles. The final approach demonstrated a 75% extension of the fatigue life of the modified CFRP, as the healing cycle after each interruption slightly recovered the modulus of the fatigued sample and delayed the ~~damage~~ progression of damage in ~~of~~ the composite structure. The composite withstood 56,000 cycles using the interrupted healing cycles without deterioration of the in-plane mechanical properties of the composite. This provides an example of the utility of intrinsic methods to retard fatigue damage. In addition, reversible dynamic cross-linking boron compounds have been utilised to retard fatigue damage in a low temperature environment and is discussed in section 3.4.

Formatted: Font color: Dark Red

3.4 Underwater or high humidity self-healing

Polymeric materials that can self-heal underwater or in high humidity conditions are in high demand to satisfy a range of industrial requirements. For instance, polymer concrete insulators have found use in the ocean environment by virtue of their high strength, inherent corrosion resistance and extremely low permeability, as well as their low cost of manufacture.[49] However, there have been no reports on these materials with regards to self-healing. These materials are used as insulating materials for solid-rigid cables, cable joints and submarine cable terminator applications in ocean environments and are expected to last over 40 years. Incorporating self-healing into such structures is therefore of interest since it can help extend the lifetime of service as well as reducing any potential defects. However, underwater self-healing can be challenging as water disrupts traditional non-covalent bonds. The hydrophilicity of water molecules and their sorption into polymer structures promote polymer plasticization. In addition, the change in the *pH* of water or polymeric swelling can weaken the mechanical

properties of the polymer. Efforts to tackle these challenges aims to use new types of dipole-dipole interactions and catechol-functionalized polymers with metal coordination among other techniques.[50, 51] This section will discuss the progress made in this area coupled with their apparent limitations.

In environmental bodies of water, the *pH* of the water varies due to natural and manufactured factors. Acidic water is ubiquitous due to natural acidification, industrialization and mines among other things. Acid rain (precipitation below *pH* ~ 5.0), a result of pollution, is an example of a manufactured occurrence which decreases the *pH* of water. It is necessary to factor in the local *pH* when designing underwater self-healing materials, proposing an additional challenge.

To circumvent these challenges, Xia *et al.* synthesised a hyperbranched polymer with multiple hydrophilic and hydrophobic terminal groups which possessed the ability to self-heal under water, more favourably in a low-*pH* environment.[50] The lipophilic polymer was made of hyperbranched polyurethane (HBPU), mercaptosuccinic acid (MSA) and acrylonitrile-butadiene-styrene copolymer (ABS). The hydrogen bonds between MSA units and the hydrophobic entanglement between ABS chains built up reversible crosslinks within the polymer networks, see Figure 11. These contributed to the strength and self-healing ability of the polymer. In addition, the hyperbranched structure enabled easy macromolecular movement in water. Water absorption of the polymer decreased with decreasing *pH* due to the increasing hydrophobicity of the system with increased protonation of the mercaptosuccinic acid. The acidity of the water was utilized to be beneficial to the process. Polymer samples were healed for 24 hours underwater and the healing efficiencies were reported as 87%, 65% and 48% with respect to tensile strength for *pH* 4, 7 and 9, respectively. This work demonstrated the use of both hydrophilic and hydrophobic interactions to create a high performance self-healing polymer with affinity towards low-*pH* environments which could be applied to sealing

elements, flexible hosepipes and linings. However, the long-term stability of the polymer matrix in ~~the~~ different water conditions and ~~the~~ surface ageing remains a challenge~~,~~; this is likely to be due to the hydrogen bonding present in the system.

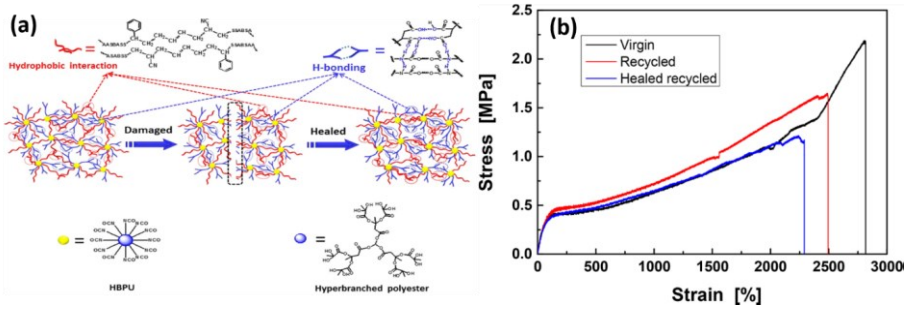

Figure 1~~1~~2 (a) Proposed self-healing mechanistic pathway for HBPU-MSA-ABS in acidic water; (b) Reclaiming effect of HBPU-MSA-ABS in water at pH = 4. Reproduced with permission.[50] American Chemical Society, 2017.

Cao *et al*. later developed a system which consisted of poly(vinylidene fluoride-co-hexafluoropropylene) (PVDF-HFP) as the base polymer to build underwater self-healing polymers which could heal at the extremities of both acidic and basic conditions, as well as in air.[52] The system possessed strong dipole-dipole interaction bonding constants between the C-F bonds due to the electronegativity of fluorine. This provided the material a significant ionic character, removing the need for metal cations or ionic components that are likely to be affected by water molecules. In addition, the C-F bond possessed a strong electrostatic nature rendering a poor hydrogen bonding acceptor, decreasing the effects of the water environment. Hence, this polymer system showed a resistance to bond disruption in water due to the large amount of C-F bonds present. With regard to self-healing ability, a dibutyl phthalate plasticizer was used to reduce the T_g of the PVDF-HFP. This plasticizer was highly hydrophobic and compatible with the polymer, and was therefore stable in water. The polymer exhibited healing efficiencies of 22% and 30% when healed underwater with respect to fracture toughness at 3

and 24 hours of healing, respectively. These values were similar to those recovered from healing in air and in extremely acidic ($pH \sim 1.3$) and basic ($pH \sim 13$) waters for the same amount of time. Whilst the healing efficiency values are seemingly lower, they are stable in much harsher aqueous environments of extremely acidic and basic conditions, whilst ~~still~~ continuing to perform consistently in air and seawater. It was demonstrated that the polymers exhibited similar surface ageing in both air and water, however the swelling of the polymer system remains a concern for its applications.

Polymeric swelling can lead to adverse effects on material properties by reducing the integrity of the chemical bonds. To combat this, Yoshie *et al*. used catechol functionalised acrylate polymers to prevent water uptake to reduce swelling-induced mechanical instability and improve self-healing functionality.[53] As shown in Figure 1~~2~~3A ~~(a)~~, after coordination with common Ca^{2} or Mg^{2+} in seawater, the resultant metallopolymers showed enhanced mechanical toughness of 5 MPa (MJ m^{-3}) and self-healing efficiency of ~80% without obvious swelling due to the metal-catechol complexes and catechol-mediated interfacial hydrogen bonding.[53] This concept was improved by using p-phenyldiboronic acid (PDBA) as a cross-linker for the poly(dopamine acrylamide-co-n-butyl acrylate) polymer through non-ionic borate ester bonds[54], see Figure 1~~2~~3B ~~(b)~~. The P-PDBA swelled only up to 2 wt% after three days of being submerged in seawater. This marginal swelling was key to its self-healing ability since the absorbed water slightly shifts the equilibrium dynamics of the esterification between catechol and boronic acid surface groups towards hydrolysis. The exposure of free catechol and boronic groups on the fracture surface leads to the formation of boronate ester bonds by esterification. The healing efficiency was reported to be 91% after three days of being submerged in seawater. This work demonstrated the potential of the catechol-based system with high self-healing efficiency and long-term stability, which is suitable for use in marine-based industries and applications.

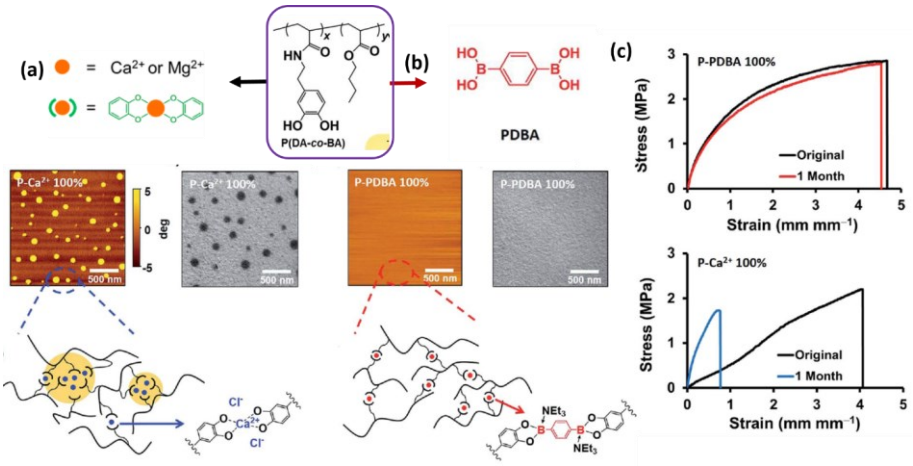

Figure 12 (A) Ionic crosslinking of catechol containing poly(dopamine acrylamide-co-n-butyl acrylate), P(DA-co-BA) using Ca^{2+} or Mg^{2+} ions; the AFM and TEM images show the ionic clusters. Adapted with permission.[53] American Chemical Society, 2016. (B) covalent crosslinking of P(DA-co-BA) with covalent boronate ester bonds; (C) Long-term stability in seawater, comparison of the tensile properties of P-PDBA and P-Ca^{2+} films incubated in seawater for one month. Reproduced with permission.[54] Royal Society of Chemistry, 2017.

In addition, the development of acid rain can reduce the *pH* of the water environment. Similarly, salt and other particulates can also lead to a corrosive environment~~s~~ in a water body and should be ~~of~~ consider~~cdation~~ when developing self-healing materials that need to operate underwater. Liu *et al.* synthesized a graphene-epoxy supramolecular elastomer with intrinsic underwater self-healing and anticorrosion properties.[55] Adamantane glycol diglycidyl ether (ADGDE) and ethylenediamine-β-cyclodextrin (EDA-CD) were synthesized and reacted with graphene oxide nanosheets to form the graphene-epoxy nanocomposite coatings, as seen in Figure 134. The self-healing properties of the material are a result of the dynamic host-guest interactions between cyclodextrin on the graphene surface and adamantane on the polymer chains. The anti-corrosion properties were attributed to the impermeability of the graphene nanosheets, which prevent electrolyte penetration whilst improving healing efficiency for the composite coating.

The self-healing properties of the material was evaluated through localized electrochemical impedance spectroscopy testing, whereby scratches were introduced into the material to expose the steel surface substrate, which was then immersed in 3.5 wt% NaCl solution. The results suggested that after 24 hours of immersion, the self-healing properties of the reinforced elastomer coatings prevented corrosion propagation and reduced localized corrosion activity at the exposed surface. The development of self-healing in corrosive extreme environments is discussed in more detail in the following section.

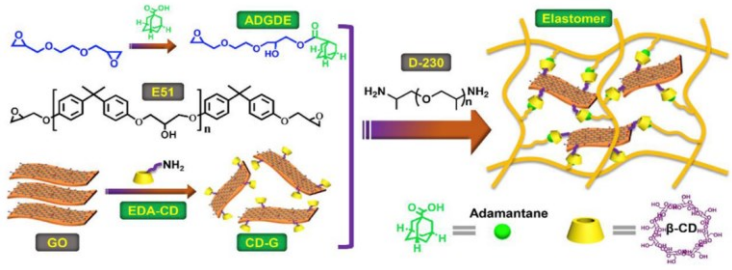

Figure 134 Fabrication pathway for epoxy-based graphene nanocomposites. Reproduced with permissions.[55] Elsevier, 2019.

3.5 Self-healing in corrosive environments

Corrosion is the deterioration of metallic structures as a result of chemical or electrochemical reactions with their environment. For example, aluminium alloys suffer from pitting corrosion in environments containing chloride since alloying elements such as Cu, Mg and Al form intermetallic phases and initiate localized corrosion reactions, thereby forming pits.[56] The corrosion process is catalysed by humidity and acidic environments due to the presence of ions. A barrier coating is often applied to protect the metal surfaces from direct contact with environment, block the penetration of moisture or oxygen to the substrate surface, or even release corrosion inhibitors to slow down the corrosion process. However, coatings can easily lose these functions once they are pierced, cracked, or scratched, and a self-accelerating

corrosion process can initiate from the metal surface as a result of an ~~the~~ attack by moisture or corrosive ions, which make it difficult to predict and prevent. Anti-corrosion coatings with self-healing functions that are able to sustain external attacks such for UV, moisture, oxygen, heat or a corrosive environment, as well as have additional functions such as self-cleaning, *pH*-sensing, or anti-fouling are in high demand. Frequently, these functionalities are complementary to each~~one~~ ~~an~~other.[57]

Self-healing anticorrosion coatings are often based on an extrinsic self-healing mechanism and have been explored in sol-gel hybrid coatings and polymeric coatings, such as epoxy or polyurethane based composite coatings. The self-healing functions can be realized by incorporation of microcapsules loaded with healing agents, or encapsulated corrosion inhibitors, which will respond and inhibit the electrochemical reactions at the exposed metal surfaces.[58] Since the use of heavy metals such as Cr (VI), Cd, Pb and Hg are strictly controlled in anti-corrosion coatings due to their toxicity and environmental concerns, corrosion inhibitors such as phosphates, nitrites, molybdates, tungstates, vanadates, borates and rare earth salts, or organic corrosion inhibitors such as benzotriazole, mercaptobenzothiazole, imidazoline, 8-hydroxyquinoline and aliphatic amines have been widely investigated.~~;~~[59] M~~m~~ore environmentally friendly inhibitors such as tannins, alkaloids, amino acids, and natural dyes have also attracted attention.[60]

A variety of types of micro-/nano-containers have been studied for controlled-release of corrosion inhibitors. Natural or synthetic clays, such as montmorillonite, layered double hydroxide[61], halloysite nanotubes (HNTs), graphene oxide, silica or polymeric capsules have often been used as nanocontainers in coatings.

For example, sol-gel silica – zirconia hybrid coatings were used to protect 2024 aluminium alloys, where the silica nanoparticles can be surface-modified by covering layer-by-layer with polyelectrolyte and inhibitor layers. When using halloysite nanotubes as the nanocontainer,

corrosion inhibitors such as benzotriazole[62], 8-hydroxyquinoline or 2-mercaptobenzothiazole[63] were loaded inside the lumen and the outer surface of the halloysite nanotube was further covered layer-by-layer with polyelectrolyte multilayers. The silica-zirconia coatings containing the nanocontainers were able to release entrapped corrosion inhibitors in response to *pH* changes, and prevented ~~the~~ corrosion ~~process~~ after 24h of immersion in a dilute saline solution, showing good self-healing properties;[64] this system therefore provided an enhanced long-term corrosion protection.

For epoxy coating protected steel substrates, a dual-loaded halloysite (HHNT) containing a primary corrosion inhibitor imidazole (IM) in the inner lumens, and coating a secondary inhibitor dodecylamine (DDA) on the halloysite surface together with polyelectrolyte multilayers were investigated. As shown in Figure 1~~4~~5, the hybrid epoxy/HHNT (3 wt%) exhibited corrosion inhibition efficiencies of 99.8% for steel substrates, compared to 92% for the coating containing imidazole-loaded halloysite. The high anti-corrosion properties of hybrid coatings are attributed to the synergetic effect of the loaded inhibitors in halloysite and their efficient release signalled by localized *pH* change of the corrosive medium. In addition, the surface coating with multilayer of polyelectrolytes improved the dispersion of the halloysite nanocontainers.[65]

Halloysite nanotubes loaded with three different inhibitors (Korantin SMK, Halox 520 and $(NH_4)_2TiF_6$) were compared in epoxy composite coatings for steel substrates. By employing a neutral salt-spray test (5% NaCl, 35 °C), the epoxy coating containing 5 wt% of inhibitor-loaded halloysite nanotubes showed improved anti-corrosion performance compared to a commercial epoxy coating containing 20 wt% of zinc phosphate. The addition of the free inhibitors into the coating without the use of halloysite nanotubes led to a deterioration of the corrosion protection level. The halloysite nanocontainer-impregnated coatings were able to sustain performance for over 1000 hours in a salt spray test.[66] When

aminopropyltriethoxysilane modified halloysite nanotubes were double-doped with Zn^{2+} and imidazole dicarboxylic acid (IDC), the modified epoxy ester coating provided a corrosion-inhibition efficiency of 90% for mild steel in 3.5 wt% NaCl solution in 24 hrs. After salt spray testing, a smaller disbonded area was observed for the scratched epoxy ester film bearing the double-doped halloysite nanotubes. The IDC acid carries two anionic carboxylic acid groups, which improved the release behaviour at an elevated *pH*, which usually occurs at cathodic sites.[67] The enhanced anticorrosion performance was ascribed to the precipitation of zinc hydroxide and a complex of Zn^{2+}/Fe^{2+}-IDC in the coating.[68]

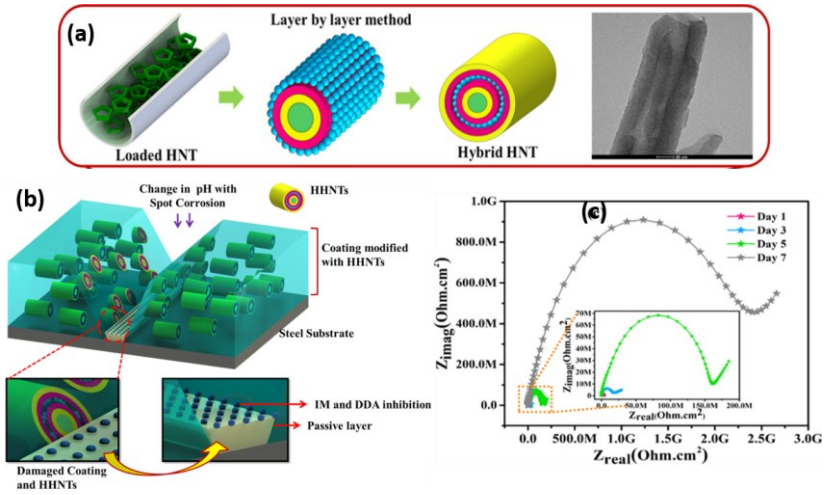

Figure 1~~4~~5. (a) Loading of corrosion inhibitors to modify halloysite (HNT) to hybrid HNT (HHNT); (b) Protective self-healing mechanism of epoxy/HHNT hybrid coatings; (c) Impedance spectroscopy results of the hybrid coatings after immersion in 3.5 wt% solution, Nyquist plot. Adapted with permission.[65] American Chemical Society, 2020.

The overall coating performance can be affected by the extent of the uptake and release of containers, the prevention of premature leakage, the compatability between the container and coating matrix, and the cost and procedure.[69] Inorganic nanoparticles show benefit in terms of a controlled release of inhibitors for self-healing protective coatings, low cost and good

mechanical reinforcement and hardness. However, their dispersion and compatibility within a polymer matrix are technically challenging for producing a homogeneous coating. In addition, the optimisation of the inhibitor loading and controlled release also require further investigation. In comparison to inorganic nanoparticles, polymer microcapsules can be designed to be *pH*-sensitive and rupture to release corrosion inhibitors in response to a *pH* change. Since corrosion leads to acidity changes on the reaction sites of the metal substrate, the aqueous solution near the cathode becomes basic due to reduction reactions of oxygen and/or protons.[69] A *pH*-sensitive microcapsule composed of a cross-linked polyester shell and containing cerium nitrate as the inhibitor was designed to release the inhibitors in response to a hydrolysis reaction.[56, 70] The under-film corrosion of a steel sheet was suppressed by addition of *pH* sensitive microcapsules to the coating matrix. The subsequent release of cerium ions was confirmed on a corroding steel surface.[70]

It has also been reported that oleyl phosphate can be used as an effective dispersant for the dispersion of poly(urea-formaldehyde)-based microcapsules in an epoxy coating.[71] A microcapsule content of at least 15 wt% was required to efficiently restore the epoxy matrix, whilst providing corrosion protection to underlying low-carbon steel when the particles were not well dispersed. However, only 5 wt% of the microcapusules are needed to obtain good self-healing and anticorrosion efficiencies when adding 0.5 wt% of oleyl phosphate as the dispersant, due to the improved dispersion of the microcapsules in the epoxy.

Recently, a self-healing graphene microcapsule-thickened oil coating was reported to form a dynamic network and improve the stability of the metal substrate. Upon the introduction of damage to the coating, the oil flows rapidly to cover the exposed area, reconnecting the particle network. The flow properties of the oil-based coatings make them applicable for surfaces with complex geometries which help form a barrier coating that is free from pin-holes, both in air

and in acidic water. The coating could self-heal repeatedly, even after scratching at the same spot 200 times.[72]

A single layer epoxy nanocomposite coating containing titania nanotubes, loaded with dodecylamine as an inhibitor, and an epoxy monomer as the self-healing agent, showed combined self-healing ability and the corrosion inhibition effect on a carbon steel. The coated steel substrates were tested before and after scratching in 3.5 wt% NaCl solution for different times of immersion. The blank epoxy coating delaminated and deteriorated after five days, while the epoxy-coated steel that contained the healing additives exhibited a decreased corrosion rate after immersion in saline water for five days. The combined effect was based on a release of the monomer, the self-healing agent, and its successive crosslinking with amine immobilized in the nanotubes, as well as the release of the dodecylamine in the loaded nanotubes. After 10 and 15 days of immersion, the degree of corrosion was not fully controlled due to the insufficient dodecylamine content inside of the titania nanotubes.[73]

Supramolecular chemistry was investigated for corrosion and biofouling prevention and has been discussed in a recent review.[74] The reversibility of supramolecular interactions offers both self-healing and responsiveness properties to coatings, although the non-covalent bonds may offset the barrier and stability of the coatings. It is proposed that partial replacement of covalent bonds with non-covalent bonds (up to 25%) may introduce a self-healing function without losing the barrier coating properties.[75] Therefore, the current status of the application of supramolecular chemistry in corrosion and biofouling prevention are mainly focused on forming microcapsules through supramolecular polymers, host-guest inclusion compounds, organic-inorganic hybrid materials, crown ethers or layer-by-layer assembled multilayers.

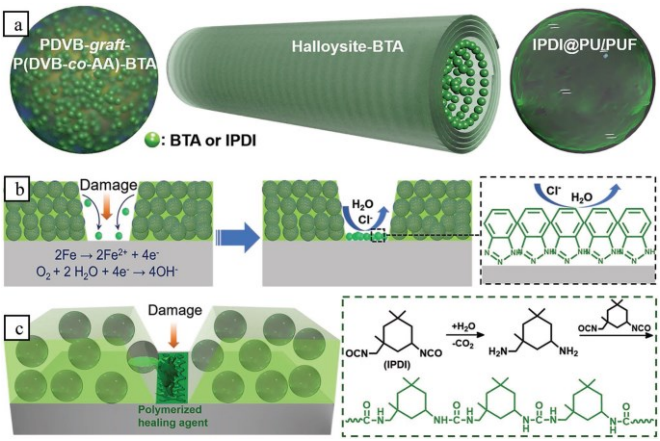

Figure 1~~5~~6 (A) Different types of self-healing nano/microcontainers used. (B) The autonomous self-healing anticorrosion coating with PDVB-graft-P(DVB-co-AA)-BTA and halloysite-BTA or (C) IPDI@PU/PUF. Reproduced with permission. [60] John Wiley and Sons, 2019.

pH-responsive self-reporting smart materials have been designed for self-healing anti-corrosion systems. [60] The self-sensing function was enabled by encapsulated phenolphthalein (phph) as the *pH* indicator, which can change colour from colourless to pink in response to a *pH* change from low (acidic) to high (alkaline) to autonomously indicate the onset of corrosion; see Figure 1~~5~~6. When corrosion occurs, the colour around cracks gradually turn~~s~~ pink over time as a result of the increased local *pH*. Monitoring of the appearance of a light-pink-colour area indicates the onset and propagation dynamics of corrosion. The poly(divinylbenzene)-graft-poly(divinylbenzene-coacrylic acid) (PDVB-graft-P(DVB-co-AA)-phph microspheres that contain a corrosion inhibitor of benzotriazole (BTA) were added to the acrylic resin coatings, and showed the highest anticorrosion efficiency. The self-sensing coating with 5 wt% of PDVB graft-P(DVB-co-AA)-phph microspheres was applied to a Q235 carbon-steel coupon, and showed better performance than BTA-loaded halloysite and polyurethane/poly(urea-formaldehyde) microcapsules filled with isophorone diisocyanate (IPDI@PU/PUF).

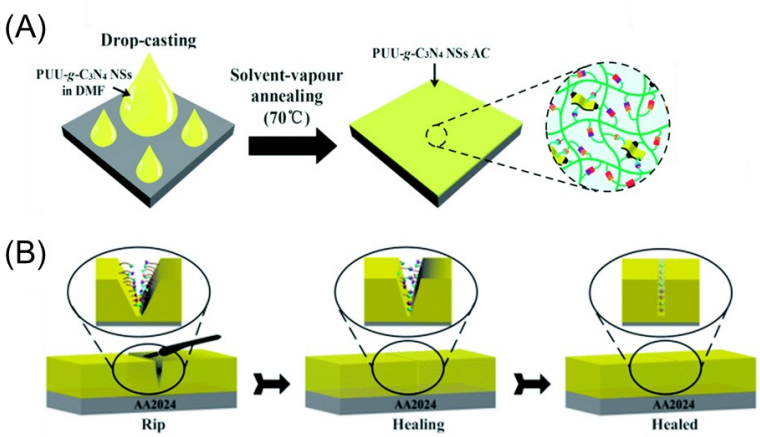

Figure 1~~6~~7 (A) Schematic o~~f~~ the synthesis of the poly(urea-urethane)–graphitic carbon nitride nanosheet (PUU-g-C_3N_4 NS) composites anticorrosion coating (AC). (B) Self-healing mechanism of the coating. Adapted with permission.[76] Royal Society of Chemistry, 2018.

Intrinsic self-healing materials have also been considered for anticorrosion coating applications. In a recent study, poly(urea-urethane)–graphitic carbon nitride nanosheet (PUU-g-C_3N_4 NS) composites were tested on an aluminium alloy 2024, as seen in Figure 1~~6~~7.[76] The poly(urea-urethane) matrix offers ambient self-healing properties due to its multiple hydrogen bonds, with the g-C_3N_4 nanosheets serving as both chemical and physical cross-linkers, ensuring the mechanical properties of the composites. The 2D layered structure of the material provides good ~~impermeability to~~ water and oxygen impermeability, which increases the corrosion resistance. The PUU-g-C_3N_4 NS coating was able to protect substrates in 0.5 M NaCl for 20 days; it could also heal a surface scratch after 10 min and recover anti-corrosion properties.

Formatted: Font color: Dark Red

Shape memory polymers are also promising for self-healing protective coatings. The challenge lies in the selection of suitable corrosion inhibitor for long-term protection without affecting coating performance, as well as the properties of the shape-memory polymer. The disadvantage

of these coatings is the extent of phase separation which can be influenced by the composition, chemical structure and phase transition temperature of the polymer.[77]

3.6 Self-healing under high vacuum

Self-healing under a vacuum or low pressure environment presents several unique challenges to self-healing materials. Firstly, their self-healing response to damage must be rapid, within seconds or even fractions of a second of the actual damage taking place since the environmental conditions maintained by the barrier material needs to be persevered upon damage. Examples where vacuum environments are important range from building materials, such as vacuum insulation panels, to aerospace environments in low earth orbit. Secondly, their self-healing mechanism must be autonomous upon the introduction of damage. Autonomy is needed since the location of damage may be inaccessible, and the time required to repair the damage needs to be as fast as possible.[78]

As a result, three routes have been explored to date, which includes an *oxygen dependent* approach, an *oxygen independent* approach and a *thermal* approach. The oxygen dependent approach utilises oxygen that is leaking between environments from impact damage to initiate a polymerisation reaction to seal the hole. Zavada *et al*. used oxygen-initiated thiol-ene reactions between trialkylborane resins to polymerise immediately after the introduction of a puncture. Under an atmospheric oxygen atmosphere concentration (21%), the polymerisation reached 80% conversion within 30 seconds.[79] The healing mechanism involves oxygen that reacts with the tributylborane to form alkyl and alkoxy radicals. These radicals propagate the thiol-ene reaction by reacting further with trialkylboranes.[80] Due to the sensitivity of tributylborane to oxygen, the rate of the reaction was high, reported as 1.5×10^8 M^{-1} s^{-1}.

Further testing by placing the trialkylborane resin in a tri-layered structure was investigated to simulate a spacecraft wall. The tri-layered structure was subjected to a ballistic~~s~~ puncture to

simulate impact and puncture formation from a micro-meteoroid or small space object. Upon immediate impact of the projectile, the thiol-ene reaction was initiated by atmospheric oxygen. This meant that none of the trialkylborane resin was observed as spray as the projectile left the tri-layered structure, indicating that the reaction had proceeded sufficiently rapidly to solidify the resin before the projectile had finished passing through the structure. Thermal analysis during and after the impact showed that the temperature of the impacted area remained elevated due to the subsequent polymerisation reaction taking place, as seen in Figure 1~~7~~8.[79]

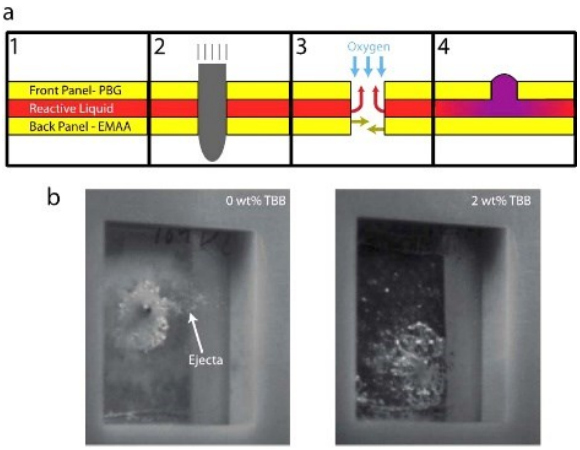

Figure 1~~7~~8 Top: Schematic of the ballistics projectile testing set up and expected result. Middle: Ballisitics projectile testing result images. Reproduced with permission.[79] American Chemical Society, 2015.

The second approach uses an oxygen independent pathway and utilizes either a curing agent or an acid catalyst to heal a puncture. A curing agent is able to react with the epoxy structure to seal a hole and prevent any further loss of vacuum. This can be implemented for vacuum insulation panels using a five layered structure, using a separator to prevent the epoxy and the curing agent from prematurely reacting, as shown in Figure 1~~8~~9.[81] Vacuum insulation panels

are building materials which help improve the heating efficiency of buildings due to a higher thermal resistance compared to traditional building insulation materials.[82] However, once damaged by accidental cuts in service or during installation, the subsequent loss of the vacuum within the panel leads to a loss of their insulation properties.[83]

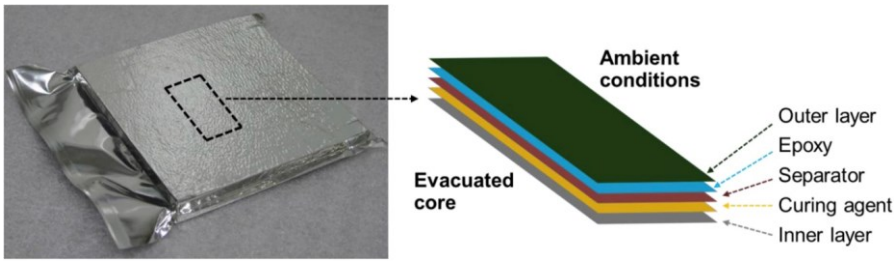

Figure 1~~8~~9 A Vacuum insulation panel and a schematic diagram for the self-healing vacuum insulation panel. Reproduced with permission.[81] Elsevier, 2019.

As an example, an Epon 8111 structure using a poly(ethyleneimine) curing agent was utilised in a vacuum insulation panel. The vacuum panel was punctured using either a needle or a screw and upon puncturing with a needle, the air pressure inside the vacuum increased as the needles were hollow, allowing air leakage. However, in both cases where a needle and a screw was used, self-healing was able to take place within ten seconds to prevent further air ingress to the vacuum panels.[81]

In addition, microvasularised polymer sheets containing two microvascular networks were designed to self-heal by combining two epoxy resins, 2-hydroxyethyl methacrylate (HEMA) and 2-hydroxyethyl acrylate (HEA), with an acid catalyst. In addition, whilst the vascular system was designed to heal larger macroscopic cracks, a microcapsule network was also established using the same system to heal smaller microscopic cracks, as seen in Figure 19~~20~~. Upon rupture, a gel was formed rapidly within 30 seconds. However, a further 1 to 3 hours was required for polymerisation to take place between the two groups. During seal testing, samples

were left for 24 hours before retesting their ability.[84] Whilst a 100% recovery was achieved, the long time frames required for this system to self-heal fully prevents its use in time-critical situations, such as on air- or space-craft.

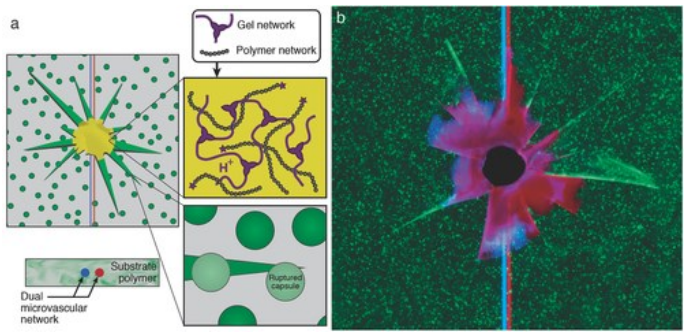

Figure 1920 (a) Schematic for microvascular and microcapsule based HEMA:HEA self-healing system. (b) Optical microscopy image from projectile damage for the dual hybrid self-healing system. Reproduced with permission.[84] John Wiley and Sons, 2019.

Another route to self-healing under vacuum environments is to utilise a thermal approach to polymerise and seal damage due to atomic oxygen in a low earth orbit environment. Atomic oxygen can degrade materials by breaking covalent bonds due to their high energy.[85, 86] This is particularly useful in the case of spacecraft where the temperature on the surface of the spacecraft can fluctuate between -100 °C to +100 °C depending on whether the space craft is in the earth's shadow or not.[85, 87] Therefore, atomic oxygen resistant 2-ureido-4[1H]-pyrimidinone (UPy) functionalised polyhedral oligomeric silsesquioxane (POSS) coatings were developed by Wang *et al*. The UPy groups exhibited four potential hydrogen bonding sites, allowing temperature dependent self-healing to be utilised.[88]

At 80 °C, the hydrogen bonds could be overcome so that they could break and then reform upon cooling to heal cracked surfaces from damage to the coating. A maximum crack width healing of 1.1 µm was found when subjected to 100 °C for 2 minutes. Due to the dynamic

interactions present for self-healing, the UPy-POSS coating was found to be able to undergo multiple self-healing cycles.[88]

Overall, research into self-healing under vacuum environments is still in its early infancy. Nevertheless, a range of routes to solving this problem have been put forward to provide self-healing in high vacuum conditions. Since sending spacecraft and low earth orbit satellites into space is becoming increasingly more common, it is of particular interest to the aerospace industry to develop autonomous self-healing systems for impact-based damage and atomic oxygen based damage, as well as from UV degradation and thermal cracking.

3.7 Self-healing under high intensity UV radiation

Long term exposure to ultra-violet (UV) radiation can lead to significant degradation of a large range of materials. UV radiation can result in photo-oxidative degradation that leads to breaking of polymer chains, production of radicals, reduction in molecular weight and causes deterioration of mechanical properties after an unpredictable amount of time.[89] Polymeric materials are used for infrastructure and vehicle applications due to their low cost and ease of manufacturing, where they are exposed to solar radiation. This radiation is particularly more harsh in a space environment, where there is no stratosphere filter for higher frequency or shorter wavelength UV radiation; this can commonly induce the formation and propagation of microcracks in polymeric materials.[90] The extreme environment in this sense refers to an environment in which there is constant exposure to UV radiation. Researchers have developed methods to combat UV-triggered degenerative processes by taking advantage of light as the self-healing source, this is particularly important in situations where human intervention is inconvenient. Photo-crosslinking reactions, photoinduced metathesis and material heating are some possible effects of light irradiation that can initiate the self-healing process.[91] The advantages of light-stimulated self-healing include an ability to operate

remotely/autonomously, low cost and it can exploit readily available light sources to provide localized healing whereby damaged areas can be repaired without disrupting undamaged areas.[92, 93]

The use of UV to act as the self-healing mechanism for extrinsic healing using microcapsules has been reported widely, and can be used to heal either UV induced degradation or mechanical damage. Guo *et al.* encapsulated an epoxy resin and a cationic photo-initiator into a single SiO_2 microcapsule through a combined interfacial/in situ polymerization strategy, which was embedded into an epoxy resin coating.[90] Microcrack formation from UV light led to microcapsule rupture, leading to the release of the epoxy resin and photo-initiator simultaneously due to a capillary effect which subsequently fills the crack. When irradiated, the epoxy groups are consumed due to their ring-opening reaction. There was an 89% conversion of the epoxy groups in 30 minutes of radiation. This self-healing system also showed resistance to long-term thermal cycling which is significant for aerospace applications. Furthermore, this form of UV-triggered cationic polymerization mechanism is insensitive to atomic oxygen that is prevalent in space environments.

Song *et al*. mixed microcapsules with a coating matrix formulation that was prepared by sol−gel reaction of tetraethyl orthosilicate (TEOS), in the presence of a polysiloxane, to create a self-healing coating formulation.[94] The microcapsule was based on an encapsulated methacryloxypropyl-terminated polydimethylsiloxane (MAT-PDMS) and benzoin isobutyl ether (BIE) photoinitiator with urea-formaldehyde polymer. Upon mechanical damage, the region was filled with the healing agent that solidified upon sunlight irradiation. The self-healing efficiency was evaluated with water permeability and chloride ion penetration tests. For the water permeability test, the cracked self-healing coating was exposed to sunlight for 4 hours prior to water immersion. The water uptake corresponded to ~~was~~ 10% of that compared to the cracked control coating sample that had no sunlight exposure. For the chloride ion

Formatted: Font color: Dark Red

penetration test, a scribed self-healing coating was exposed to sunlight for 4 hours and an electrical potential was applied to the material to measure the current from the movement of chloride ions. The scribed self-healing coating demonstrated a current almost four times lower than the current of the scribed control sample, demonstrating its ability to self-heal in sunlight. The use of direct sunlight instead of a specific range of UV-radiation is beneficial to any application involving outdoor use. Further work is needed on more extensive long-term studies to understand how many healing cycles these coatings can withstand.

A second method to induce light-stimulated self-healing involved the use of UV-triggered self-healing polyurethanes with photo-reversible coumarin moieties. Coumarin derivatives undergo a [2 + 2] cycloaddition when~~upon~~ exposu~~re~~d to long-wave UV irradiation (365 nm), and this process ~~can be reversed~~ is reversible using short-wave UV light (254 nm) as shown in Figure 20~~1~~A.[95] Ling *et al*. synthesized a polyurethane consisting of isophorone diisocyanate, polyethylene glycol and 5,7-bis(2-hydroxyethoxy)-4-methylcoumarin to take advantage of the reversible photodimerization and photocleavage habit of coumarin and induce self-healing in the polyurethane with repeated crosslinking and de-crosslinking~~, as shown in Figure 21Aa~~.[96] When the polyurethane was irradiated with 350 nm UV light, the double bonds of 4-methylcoumarin gradually dimerized to form cyclobutane rings, resulting in destruction of the conjugation between the double bonds and phenyl groups, see Figure 20~~1~~. Conversely, when the polyurethane was irradiated with 254 nm UV light, the cyclobutane derivatives are recovered to 4-methylcoumarin monomers, decreasing dimerization. To evaluate the self-healing properties, room temperature tensile tests were conducted on the initially cross-linked (350 nm) polyurethane specimens. After failure, 254 nm UV light was irradiated upon the fractured surfaces immediately. The authors noted optimal healing conditions of 1 minute of 254 nm UV radiation and then 90 minutes of 350 nm illumination. Under these conditions, a polyurethane specimen with tensile strength of ~1.2 MPa was able to self-heal with efficiencies

Formatted: Font color: Dark Red

of 100%, 90% and 61% after three successive tensile measurements, with respect to tensile strength. However, increasing the ratio of coumarin led to a higher tensile strength (~3.6 MPa) at the cost of a lower self-healing efficiency, namely 68%, 29.4% and 21% after three successive tensile measurements with respect to tensile strength. There is a greater restriction on chain mobility with increased coumarin content; this reduces chain entanglement necessary for effective self-healing. Overall, this work demonstrated a method to utilize light to induce self-healing in polymeric materials that would be suitable for structural application.

More recently, Wang *et al.* adapted coumarin-based polyurethanes to synthesize UV-induced self-healing materials with significantly higher tensile strength and tensile strain to failure for applications in self-healing coatings, electrochemical sensors and electronic skins, as shown in Figure 2~~0~~1B~~b~~.[97] A range of polyurethanes was synthesized with 4, 4′-methylenebis (phenyl isocyanate) (MDI), poly (tetramethylene glycol) (PTMEG) and 4-methylumbelliferone (coumarin derivative). Optimal healing conditions of 10 minutes of 254 nm UV radiation and then 300 minutes of 350 nm UV radiation were used. The high tensile strength (27 MPa) and strain at break (890%) were attributed to, firstly, the large number~~amount~~ of phenyl groups in the ~~MDI introduced into the~~ polyurethane due to the MDI and, secondly, the high molecular weight chain extender PTMEG which had longer flexible chains and fewer hard segments. Tensile tests on the healed polyurethane resulted in a self-healing efficiency of 71%. As the content of MDI and coumarin increased, the self-healing efficiency also increased, but at the cost of the mechanical properties. In comparison with the work of Ling *et al.,* this appears contradictory since an increase in coumarin content increased the mechanical properties and decreased self-healing efficiency. This could be related to the amount of phenyl groups present between the two works. The increase in phenyl groups in the research of Wang *et al*. result in accelerated rates of fracture and reformation of the quaternary ring, which also implies that more broken~~destroyed~~ covalent bonds were reformed. However, the research of Ling *et al.* had

Formatted: Font color: Dark Red

Formatted: Font color: Dark Red

a lower amount of phenyl groups present and increasing the coumarin content had an alternate effect, whereby the T_g of the material increased and the average molecular weight between crosslinks of the photo-crosslinked polyurethanes decreased, thereby reducing chain entanglement but raising mechanical strength. Nevertheless, the high tensile stress and strains combined with good elasticity shown from cyclic tensile tests demonstrate its potential application in the fields of smart materials, including self-healing electronic skins, coatings and electrochemical sensors and devices.

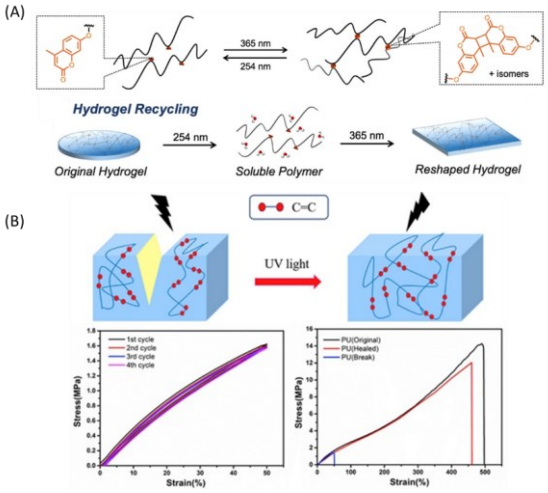

Figure 2~~0~~(A~~a~~) Reversible photodimerization and photocleavage reactions of coumarin moieties upon UV light irradiation of 365 and 254 nm, and reprocessability of hydrogel formation. Reproduced with permission ~~from ref.~~[95] American Chemical Society, 2018. (B~~b~~) Schematic diagram for self-healing in coumarin based polyurethanes, with both cyclic loading and unloading and self-healing results shown. Reproduced with permission.[97] Elsevier, 2019.

A criticism in the use of UV-triggered self-healing of the coumarin moieties exists within the notion that specific wavelengths are needed. Outdoor healing materials are exposed to broad wavelengths induced from the sun. In addition, there can be difficulties to offer relevant instrumentation to achieve on-demand healing in outdoor circumstances using specific

Commented [A1]: (Reference 102 does not contain this figure)?

Formatted: Not Highlight

Formatted: Not Highlight

Formatted: Not Highlight

wavelengths of UV light. To circumvent this challenge, Fang *et al.* reported a sunlight-induced self-healing epoxy coating due to the photothermal effect, through the introduction of the diamine of m-xylylenediamine (MXDA) as curing agent, monoamine of 4-(heptadecafluorooctyl)aniline (HFOA) as hydrophobic chain extender, and aniline black (AB) as organic photothermal compound for sunlight into the diglycidylether of bisphenol A (DGEBA) epoxy network.[93] Using a spincoating reaction method, MXDA was gradually replaced by HFOA to reduce T_g and crosslinking levels of the epoxy network. This~~,~~ enabled~~ing the~~ thermally induced self-healing ~~at a temperature~~ above the T_g on the basis of crack closure, ~~as well as~~ chain diffusion and re-entanglement. The addition of aniline black as a photothermal filler enables the material to transform light energy to localized heat. The self-healing efficiency was evaluated using a method based on image analysis and found self-healing efficiencies of 83% to 91% after 10 minutes of focused simulated sunlight irradiation. Furthermore, the self-healing was demonstrated outdoors upon a coating sample with a common handheld magnifier using the sun for 10 minutes that showed visible evidence of scratch healing. This work demonstrates the convenience of common items to induce light-stimulated self-healing for outdoor applications. However, the image analysis technology used is qualitative and unable to be related to the physical and mechanical properties of the coatings as it is based on digital quantitative processing and warrants further investigation.

Formatted: Font color: Dark Red

Ambient sunlight was also used for a self-healing sensor skin fabricated on a substrate of copper-clad polyimide sheets in a layer-by-layer technique using polyimide sheets and an ultraviolet (UV)-curable epoxy by Carlson *et al.*[98] The UV-curable epoxy was used as both a structural adhesive and as a self-healing filler material. The UV-curable epoxy was released and healed by ambient sunlight when the skin was damaged.

As an alternative approach, light stimuli can also be used as an effective trigger for the shape-memory effect in polymers.[99] The temperature of a given shape-memory polymer governs the

transition from a temporary ~~shape~~ to ~~a~~ permanent shape and the photothermal effect allows the use of light to control the shape memory effect.[91] Shape-memory polymers containing photothermal fillers are able to convert irradiated light into localized heat, as shown by Fang *et al.*[93] Examples of photothermal fillers include organic dyes, ligands, gold nanoparticles, gold nanorods, carbon nanotubes and graphene.[91] However, it is challenging to provide the same polymer with both light-stimulated self-healing and shape-memory due to structural incompatibilities.[99] Zhang *et al*. attempted to overcome this challenge by chemically cross-linking a crystalline polymer and loading it with a small amount of gold nanoparticles.[99] The photothermal effect controlled the shape memory process by tuning the temperature of the crystalline phase and activated the self-healing process through crystal melting and recrystallization. A film of an initial defined shape was stretched at 80 ºC to 400% strain, which was followed by cooling to room temperature to fix the temporary shape. The permanent shape was recovered following ~~exposure to a~~ exposure to a laser beam ~~exposure~~ with a~~of~~ wavelength of 532 nm. To evaluate self-healing efficiency, tensile tests were performed on the original and optically healed samples. The authors reported a self-healing efficiency of 62% with respect to tensile strength after only 3 seconds of laser exposure. The healing could also be repeated several times. In addition, the researchers were able to show that the self-healing and shape memory effects can be executed in a sequential manner via a folding and cutting method, as shown in Figure 2~~1~~2. Laser beams of ~7 W/cm^2 could promote shape recovery without triggering healing, whereas beams of ~13 W/cm^2 could trigger the healing without promoting shape recovery. This work highlights another advantage of light utility to promote self-healing and shape-memory.

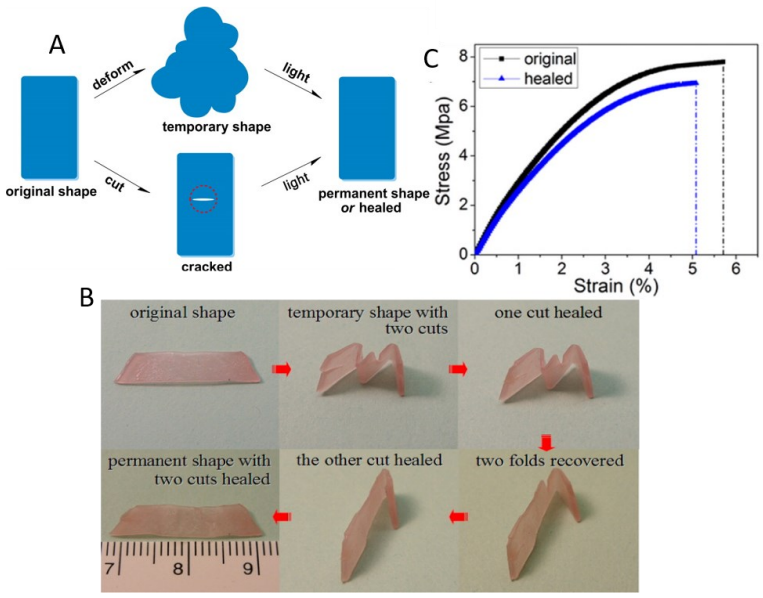

Figure 2~~1~~2 Optical healing and the light-controlled shape recovery process for a cross-linked film. (A) Schematic of light-triggered shape memory and healing exhibited by a same polymer. (B) A cross-linked film of PEO/AuNP with optical healing and light-controlled shape recovery processes sequentially triggered. (C) Stress versus strain measurements of the original and optically healed film. Reproduced with permission.[99] American Chemical Society, 2013.

More recently, Bai *et al.* proposed a thermoset polyurethane/graphene oxide composite with light-induced shape memory effect, solid-state plasticity and self-healing performance.[100] Polycaprolactone was grafted onto graphene oxide by ring opening polymerization of ε-caprolactone before crosslinking with aromatic diisocyanate to facilitate the formation of a polymer network structure. The graphene oxide provided the composite with near infra-red light-induced shape memory and light-induced plasticity due to its high photothermal conversion efficiency. Similarly, crack interfaces on damaged samples could be closed during irradiation by near infra-red light due to shape memory effects. After irradiation for 30 minutes, polymer chains diffused across the damaged interface along with carbamate exchange reactions,

Formatted: Font color: Dark Red

leading to topological rearrangement of the polymer networks, resulting in self-healing. The authors reported a self-healing efficiency of 85% with respect to tensile strength after 30 minutes of near infra-red light irradiation. The material possessed a high tensile strength of 16.6 MPa and the authors displayed its reconfigurability and corrosion resistance features, demonstrating its suitability for applications in light control actuators, self-healing coatings and as an optical welding material.

The examples above have a common link with use of lasers to drive the self-healing and shape memory processes. Wu *et al*. developed an ultrafast infrared laser driven self-healing nanocomposites and demonstrated their application in flexible electronics using Diels-Alder chemistry (PU-DA) based composites linked with functionalised graphene nanosheets (FGNS).[101] The mechanical properties of the material were restored with more than 96% healing efficiency after 1 minute of irradiation by 980 nm infra-red laser after mechanical damage. This provides a novel solution for next generation intelligent flexible electronics where light-driven hydrogel actuators show a number of advantages in flow control, soft robotics and microreactors. Similarly, Cheng *et al.* developed a photothermal responsive and self-healing nanocomposite hydrogel containing poly (N-isopropylacrylamide) (PNIPAM) and poly (N,N-dimethylacrylamide) (PDMAA), ~~to~~ serving~~e~~ as light-driven valves that~~by stimulating~~ stimulate the bilayer and the "hinge-type" hydrogel composites.[102] Using graphene oxide (GO) and clay, the hydrogels possess good mechanical properties and near-infrared-driven self-healing behaviour ~~because of the~~due to non-covalent bonding between the polymer chains and clay. The "hinge-type" hydrogel presented repeatable deformation with irradiation, which has been demonstrated using a light-driven self-healing valve.

Other researchers have used materials based on metal coordination to harness UV light-controlled polymers. Borré *et al.* reported on a series of metallopolymers based on zinc(II)–terpyridine coordination nodes that ~~, and~~ bear~~ing~~ photoisomerizable diazobenzene units and/or

Formatted: Font color: Dark Red

Formatted: Font color: Dark Red

Formatted: Font color: Dark Red

solubilizing luminescent phenylene–ethynylene moieties.[103] These supramolecular polymers can act as powerful gelating agents at low critical gelation concentrations, and exhibit UV light-triggered mechanical actuation and luminescent properties, ~~which was~~ exemplified by a light-powered self-healing soft actuator. Qin *et al.* fabricated anisotropic hydrogels that composed of highly ordered lamellar network cross-linked by the metal nanostructure assemblies.[104] Due to the dynamic thiolate-metal coordination as healing motifs, the composites exhibited rapid and efficient multi-responsive self-healing performance under near-infrared irradiation and low *pH* conditions.

A novel class of photo-plastic polyurethane elastomers based on dynamically covalent cross-linker hexaarylbiimidazole (HABI) and permanent cross-linker glycerol was designed and synthesized by Xiang *et al*.[105] Under the dual action of light and stretching, the photo-plastic elastomer exhibited reversible elongation and contraction-like springs. Two damaged samples were healed understand irradiation (405 nm irradiation) at room temperature, providing a solution to self-healing soft actuators for severe irradiation environment.

Overall, research into light-induced self-healing has made significant progress in converting a damaging source of UV radiation, into an asset to initiate healing. As environmental and space environmental resistance is becoming ever more prevalent for newly emerging technologies, so too are the needs to synthesise materials that take advantage of light-inducing abilities.

3.8 Self-healing under high electric field conditions

The presence of microcracks and defects in a polymer can lead to electrical treeing under the presence of an electric field, ~~causing~~ leading to short service lifetimes and failure ~~and short service lifetimes~~.[106] The electric field at which electrical treeing propagates can be hard to predict, leading to failure at a much lower electric field than for an undamaged polymer. This is especially challenging for high voltage cabling, such as undersea power cabling or within

modern aircraft. Modern aircraft contain up to 200 miles of cabling, and severe damage is caused through vibrations, flexing and salt corrosion. The defects caused by this damage can act as sites for failure. In addition, electrical aging of the protective polymer sheath can occur, creating free radicals within the polymer and propagating the failure of the polymer.[107] This was shown to be inhibited in oxygen free environments as molecular oxygen assists with free radial degradation.[108]

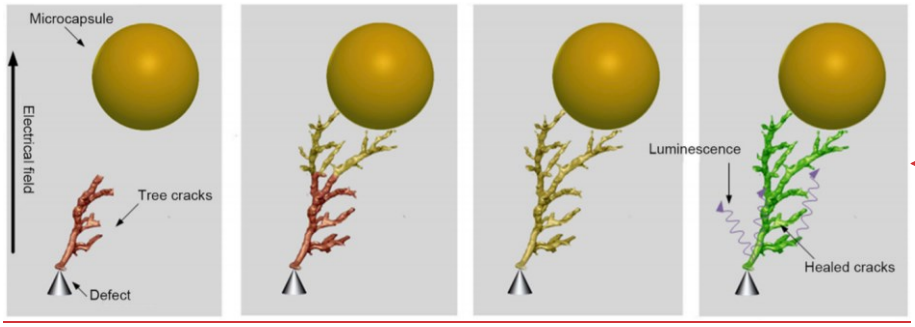

Figure 2~~3~~ Schematic of the rupturing of microcapsules from electrical treeing. Reproduced with permission~~. Elsevier, 2020~~.[106] Elsevier, 2020.~~from Lesaint *et al.*~~

To date, both intrinsic approaches, through dynamic bonds, and extrinsic approaches, through microcapsules and oil based systems have been utilised to successfully recover damage initiated from electrical fields.[109] The use of microcapsules has been demonstrated by Lesaint *et al*. as a method for inhibiting electrical treeing. They introduced urea-formaldehyde based microcapsules into epoxy resin prior to casting filled with dicyclopentadiene~~, as shown in Figure 23~~. As the electrical tree propagated through the epoxy resin, the microcapsules ruptured and filled the tree. However, as noted by the authors, the ability of the healing agent to fill the cracks of the tree depends on the viscosity of the liquid, surface tension of the epoxy crack walls and the partial pressure for filling the region.[106] Thus, most of the site can be healed to delay further failure.[110] However, any unfilled regions act as sites for initiation of electrical

Formatted: Centered

Commented [A2]: Alternatives or redraw something different

Formatted: Not Highlight

Formatted: Not Highlight

Formatted: Not Highlight

treeing once more. More recently, Gao *et al.* utilized a similar strategy~~,~~ but instead capitalized on electroluminescence, generated *in-situ* during electrical treeing, to cure the healing agents released from the microcapsule rupture, as shown in Figure 2~~2~~3.[111] ~~–~~Hybrid core-shell microcapsules were synthesised via one-step Pickering emulsion polymerization between urea-formaldehyde and TiO_2, incorporating the latter to protect the bisphenol A epoxy acrylate healing agent~~s~~ from electroluminescence during electrical treeing. The luminescence was thought to arise from the recombination ~~between~~of charge carriers injected from the electrodes and ~~, in addition with~~the impact excitation of polymer molecules by accelerated electrons. In this system, Weibull breakdown voltages of the healed polymers (35.2 kV) yielded higher values than the~~ir~~ original counterparts (33.5 kV). These qualities are attractive for integration into dielectric materials for electronic and energy applications.

As an alternative to microcapsules, a naturally derived 'drying oil' from alkyl benzene fluid and tung oil was demonstrated by Basu *et al.* which reacted upon exposure to air. The drying oil filled the space before curing and repaired the site through a curing reaction. After healing, the breakdown voltage of the healed site recovered to 85 kV m^{-1}. In addition, they proposed an unsaturated oil-based system, in which crosslinking the oil acted as the repair mechanism instead of curing. However, the crosslinking process was too slow to repair successfully cables in a real-world environment.[112]

Alternatively, an intrinsic self-healing functionality for electroactive polymers can allow them to withstand high electric fields. Dielectric elastomer actuators (DEAs) are a class of electroactive polymers that are ~~that~~ able to deform due to the electrostatic interaction between two electrodes with opposite electric charge; this was~~,~~ ~~which was~~first demonstrated in 1880 by Wilhelm Conrad Roentgen ~~by~~ who ~~spraying~~ sprayed charges onto ~~a piece of~~ natural rubber.[113] It has attracted much interest and research on actuator configurations, material properties and enhancement of actuator performance over the past decade. Structural defects occur in

Formatted: Font color: Dark Red

Formatted: Font color: Dark Red, Not Highlight

Formatted: Font color: Dark Red

Formatted: Font color: Dark Red

Formatted: Font color: Dark Red

Formatted: Font color: Dark Red

Formatted: Font color: Dark Red

Formatted: Font color: Dark Red

dielectric elastomer actuators ~~such as~~as a result of gel particles, uneven thickness, and stress concentrations which may ~~cause~~ induce dielectric breakdown ~~when a high electric field is applied~~under application on an electric field, leading to premature failure during continuous or repeated actuation, ~~and~~ reduc~~es~~ing device lifetime. Self-healing electrodes or actuators can significantly increase the ~~usage~~ lifetime of ~~the~~ dielectric elastomers, providing reliable and sustainable solutions for electronics, soft robotics, high tension cables including electric transport and future electric aircraft where altitude/low pressure environment increases the potential for partial discharge to occur.

Ultra-thin self-clearable carbon nanotube based electrodes for improved performance of dielectric elastomer actuators were developed in 2008.[114] These ultra-thin electrodes exhibit fault-tolerance in dielectric elastomers through the local degradation of carbon nanotubes during ~~dielectric breakdown~~electical breakdown ~~at a voltage of 3 kV~~under a 3 kV voltage, which can be implemented in dielectric elastomer artificial muscles and soft robots. To enable ~~enable~~ eas~~y~~e of manufactur~~ing~~ing, Michel *et al*.[115] developed a printable, ~~and~~ self-healing electrode based on 20 wt% reduced graphite nanoplatelets in silicone for dielectric elastomer actuators. ~~The actuator electrode strength could be recovered a~~After dielectric breakdown ~~voltage of under a~~at an applied voltage of 2.4 kV ~~applied voltage~~, the electrical properties could be recovered, with~~and~~ no memory or hysteresis effect ~~is~~ observed ~~in the~~ during further~~fuerther~~ cyclic actuation testing ~~and breakdown~~. ~~To achieve high strain actuation,~~ Liu *et al*.[116] developed highly conductive and compliant self-healing liquid metal electrode for high strain dielectric actuators. With the additional self-healing capacity, the dielectric elastomer actuator was more fault tolerant and resilient to ~~extreme~~ non-ideal environment~~s~~al conditions. The actuator was able to achieve a 360% strain ~~with an electrode breakdown voltage as high as to~~before the electrode brokedown ~~under a~~at an applied voltage of 3.5 kV ~~applied voltage~~, ~~with~~

highlighting potential uses in~~for~~ artificial muscle~~s~~, flexible electronics and wearable device based application~~s~~.

A new self-healing dielectric elastomer actuator was developed using a two-phase dielectric utilising an open-cell silicone sponge design that was saturated with silicone oil.[117] Upon damage, the oil flows into the voids, thereby reforming the dielectric structure. The sponge acts to hold the oil in place and reinforces stability, while the oil maintains integrity of the dielectric layer. During testing, the actuator was initially subjected to a voltage was of 3.0 kV at a frequency of 1 Hz and incrementally increased to failure at a 5 kV applied voltage. The actuator healed and the same strain was achieved after the driven voltage decreased to 3 kV within 1s. Acome *et al*.[118] utilised hydraulically amplified self-healing electrostatic (HASEL) actuators, which were able to actuate using both electric and hydraulic mechanisms. These exhibited a robust, muscle-like performance, which could repeatedly self-heal after dielectric breakdown. Self-healing grippers and muscle driven robotic arms were developed, as shown in Figure 23. The use of a liquid dielectric allowed the HASEL actuators to self-heal after dielectric breakdown. The fluctuation of the breakdown strength of the HASEl actuators was demonstrated over 50 repeatred failures, with an initial breakdown voltage of 29.0 kV, a lowest breakdown voltage of 17.5 kV and an average break down voltage of 23.8 kV. The HASEL has been successfully actuated by using a voltage of 12 kV with a frequency of 50Hz to demonstrate contraction of up to 10%, a strain rate of 900% per second, lifting more than 200

times of their own weight,[119] which has potential to be used for active prostheses, medical and industrial automation, and autonomous robotic devices.

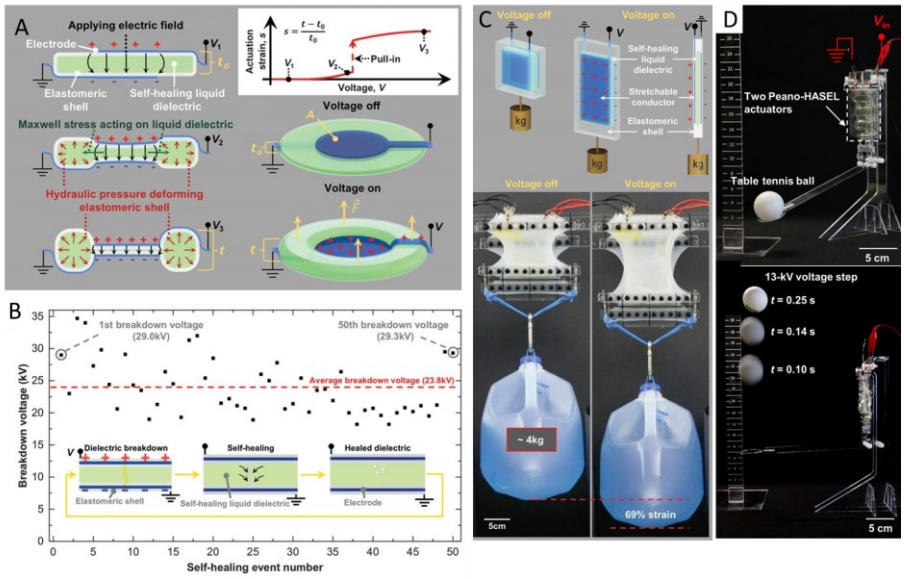

Figure 234 (A) Mechanism of a self-healable HASEL actuator, the driven voltages and its responses ($V_1 < V_2 < V_3$). With applied voltages, a donut shape deformation can be achieved for supporting an external load force *F*. Reproduced from Acome *et al*.[118] (B) Self-healing capabilities of HASEL actuators under high electric field. Reproduced from Acome *et al*.[118] (C) Mechanism of a planar self-healable linear HASEL actuator and its application of lifting heavy load. Reproduced with permission.[118] The American Association for the Advancement of Science, 2018. (D) Self-healable controllable Peano-HASEL actuators and their applications. The Peano-HASEL actuators contracted and threw a table tennis ball 24 cm into the air with a step driven voltage of 13 kV. Reproduced with permission.[119] The American Association for the Advancement of Science, 2018.

Commented [A3]: Need to pay, can we find images from other referenced papers as discussed here?

Formatted: Not Highlight

Formatted: Not Highlight

Formatted: Font: 12 pt

Formatted: Font: 14 pt

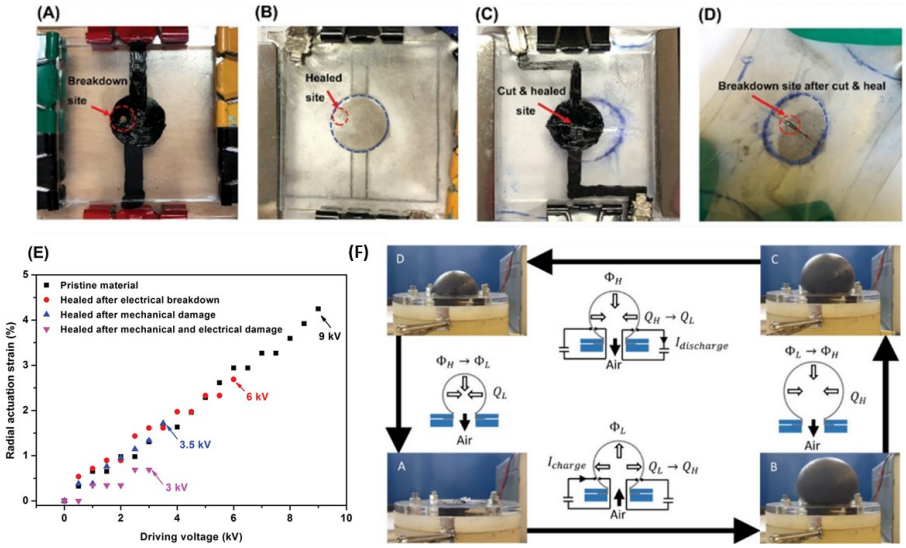

Figure 2~~4~~5. Actuator device ~~with~~ (A) after electrical failure of MG-SBS and (B) the healed breakdown site. Actuator device (C) with healed MG-SBS from mechanical damage via ~~scalpel cutting~~a blade and (D) the ~~electrical~~ breakdown failure site under an electric field of 18.1 kV mm^{-1}. (E) Radial actuation strain of MG-SBS and healed MG-SBS after electrical, mechanical, or both ~~mechanical and electrical~~ forms of damage~~s~~. Reproduced with permission.[120] John Wiley and Sons, 2019. (F) Diagram of energy harvesting cycle. Reproduced with permission.[121] American Chemical Society, 2020.

Formatted: Font color: Dark Red

Ellingford *et al.*[120] first reported self-healing dielectric actuators ~~using~~ based on a modified thermoplastic methyl thioglycolate–modified styrene–butadiene–styrene (MGSBS) elastomer, as shown in Figure 2~~4~~5. The actuator dielectric strength could be recovered by up to 67% after dielectric breakdown at a voltage of 9.25 kV, and 79% after mechanical failure, showing the potential for high field applications, ~~that~~ including soft robotics, medical devices, artificial muscles, and energy-harvesting systems. The team also reported methyl-3-mercaptopropionate grafted SBS (M3M-SBS) for dielectric actuation, which ~~provided~~ actuated with 9.2% radial

strain ~~at~~ under an electric field of 39.5 MV m^{-1} and ~~demonstrated~~exhibited ~~generated an~~an energy density of up to 11 mJ g^{-1} ~~from~~ during energy harvesting.[121, 122]

3.9 Self-healing under high magnetic fields

High magnetic field environments possess a unique challenge for self-healing polymers, since it requires a stimulus to initiate self-healing. As seen in a number of examples throughout this review, an external energy source is often required to initiate self-healing, such as heat or light, which presents a danger if additional equipment is needed to provide the energy source and a large magnetic field is present – especially if the location of the damage is in a difficult to reach or is located in obscured position.[123] Therefore, the extrinsic modification of polymers by incorporating magnetic fillers into a thermoplastic polymer matrices provides an intriguing approach to introduce self-healing in a high magnetic field environment. With regards to intrinsic modification, there is currently no work to introduce self-healing with a magnetic field stimulus and is worthy of future interest.

Under the influence of a high magnetic field, the magnetically responsive fillers vibrate and agitate, increasing the temperature inside the polymer matrix, also referred to as *Néel relaxation*.[124] Depending on the nature of the polymer, this can lead to one of two responses. Firstly, the increased temperature of the polymer can lead to surface rearrangement, surface approach and then wetting followed by chain diffusion and randomisation as time progresses during the self-healing process.[125, 126] Alternatively, the polymer can be magnetically heated to provide melting and material flow for self-healing.[127] Since the response exhibited depends on the nature and structure of the polymer, a wide range of different applications can benefit from self-healing *via* a magnetic field stimulus, including roads, inks and biomedical applications.

A thermoplastic silicone based copolymer of monomethacryloxypropyl terminated poly(dimethylsiloxane) and 6-methyl-2-ureido-4[1H]-pyrimidone-bearing methacrylate was mixed with up to 20 wt% of iron oxide (Fe_3O_4) particles via solution mixing.[128] The applied healing stimulus was an alternating magnetic field (AMF) to elastomers after 20 mins, and demonstrated a recovered tensile strain of 78% and a recovered tensile stress of 70%. The magnetic based self-healing approach showed better self-healing than directly heating the elastomers to 55 °C. This was attributed to the 2-ureido-4[1H]-pyrimidone hydrogen bonding limiting the thermo-reversibility of the polymer, indicating that a larger increase in the thermal energy is required to promote the rearrangement of hydrogen bonding, as shown in Figure 25. The success of the alternating magnetic field approach was attributed to the higher internal elastomer temperature enabling the rearrangement of hydrogen bonding.[128]

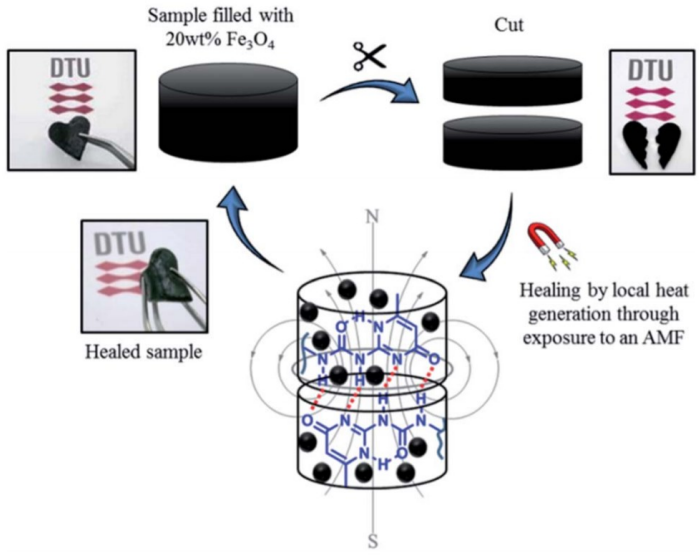

Figure 25~~6~~ Schematic of the AMF induced self-healing mechanism of monomethacryloxypropyl terminated poly(dimethylsiloxane) and 6-methyl-2-ureido-4[1H]-

Formatted: Font color: Dark Red

Formatted: Centered

Formatted: Font color: Dark Red

pyrimidone-bearing methacrylate mixed with 20 wt% of iron oxide. Reproduced with permission.[128] Royal Society of Chemistry, 2018.

Formatted: Font color: Dark Red

Formatted: Font color: Dark Red

Utilising a similar approach, $Mn_xZn_{1-x}Fe_2O_4$ particles were added to a thermoplastic poly(ethylene vinyl acetate) (EVA) matrix and manganese iron oxide coated cobalt iron oxide particles into a poly(styrene) (PS) matrix by solvent casting. In a notch test, EVA was able to self-heal 100% after damage under an application of an alternating magnetic field for 10 minutes.[125] For the poly(styrene) nanocomposites, a sample containing 10 wt% nanoparticles with a microcrack present was heated to 320 °C under an alternating magnetic field–. This initiated polymer melt flow into the microcrack, resulting in a visually observed self-healing effect.[124]

A melt mixed poly(propylene) filled with 17 nm diameter poly(ethylene glycol) coated superparamagnetic iron oxide nanoparticles was tested for self-healing in power cable applications. This also utilised Néel relaxation to dissipate heat into the surrounding polymer matrix under an oscillating magnetic field. High voltage electrical wires are at risk of electrical treeing from high, localised electrical fields leading to electrical breakdown and structural failure, destroying the device or wiring attributed.[129, 130] Prior to electrical treeing, the properties of the nanocomposite were a maximum load of 450 N and a maximum extension of 15 mm. Nanocomposites containing 0.09 vol% of modified iron oxide nanoparticles under a 15 minute oscillating magnetic field enhanced the temperature of the sample by 117 °C and led to a maximum load recovery of 100% and an extension recovery of 100%, healing the electrical treeing in the sample.

Yang *et al*. also investigated the electrical healing of the poly(propylene) samples. Prior to electrical treeing, the breakdown voltage of the superparamagnetic iron oxide containing poly(propylene) nanocomposites was 13.8 kV, and a leakage current of 5 pA. After application

of an oscillating magnetic field for 60 minutes, the poly(propylene) nanocomposites recovered 100% of both its breakdown voltage and leakage current.[130] Micro-CT scanning demonstrated how the electrical trees were healed by the oscillating magnetic field~~, see Figure 26~~. Initially, the electrical tree can be observed with many tree channels in intricate detail. During application of the oscillating magnetic field, the heat generated by the iron oxide nanoparticles initially heals the tips of the tree channels and then works inwards. Therefore, part way through the healing process only the main tree channel was left observable. After self-healing was complete, only the initial initiation site was observable.

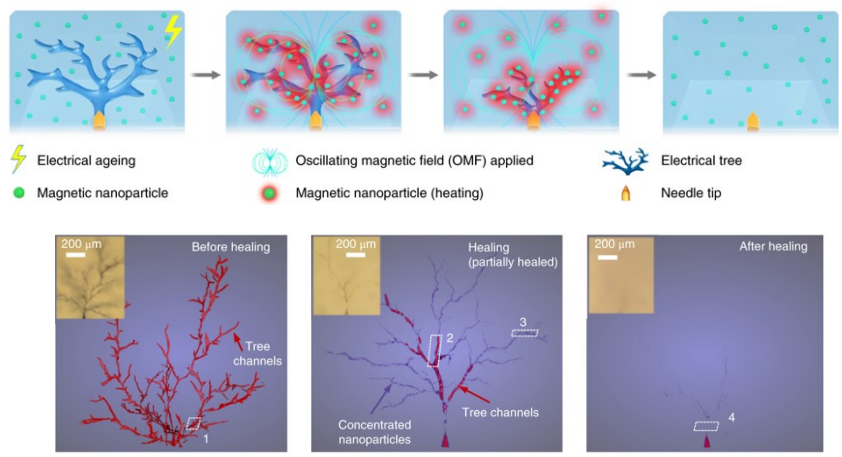

~~Figure 26 Top: demonstration of iron oxide nanoparticles oscillating under a magnetic field to heal an electrical tree. Bottom: Micro-CT images of healing of an electrical tree. Adapted from Yang *et al.*~~

Commented [A4]: Payment?
Prof Chris Bowen: I recall this image was cited in our other review' ….under electrical stress', how did you get that copyright?

An alternative application for extrinsic self-healing polymers from magnetic fields is to produce self-healing roads and pavements. By adding iron oxide or naturally occurring magnetite into bitumen the alternating magnetic field melts the bitumen that allows the polymer to flow into the microcracks present, see Figure 2~~6~~7.[127, 131] Using either solvent mixing or melt mixing approaches, bitumen based materials have shown visual crack recovery after

application an alternating magnetic field in as little as a few seconds.[131] This can reduce the likelihood of potholes or other damage to a road surface occurring and prolongs its life, reducing the need for expensive repair work.[127, 131]

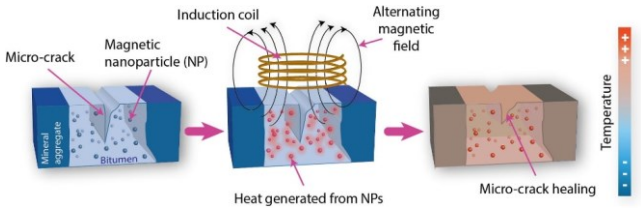

Figure 2~~6~~7 Crack healing method for bitumen containing nanoparticles under an alternating magnetic field. Reproduced with permission.[127] Elsevier, 2016.

Exploiting the shape memory properties of polymers for self-healing under a magnetic field is a novel approach to repair polymers for biomedical applications, such as coated guidewires.[132] The so called 'SMASH' polymers (shape memory assisted self-healing) enable the polymer to firstly change to its original shape under an external stimulus, which is then followed by the healing stage.[133] After failure of a poly(ethylene-co-vinyl acetate) polymer containing $Mn_{0.8}Zn_{0.2}Fe_2O_4$ nanoparticles through excessive strain, the application of an alternating magnetic field triggered a shape memory response to recover its original shape. After shape recovery, chain entanglement took place at the polymer interface for the two pieces to heal; the healing time was 10 minutes. In addition, an attached chromophore in the sample changed colour due to strain induced damage causing disaggregation of the chromophore.[132] Upon self-healing, the chromophore also returned to its original colour to provide a visual signal. The addition of a strain sensing chromophore could be utilised in general for polymers in harsh environmental conditions or when in a poorly accessible locality to demonstrate when they are under strain or beginning to fail.

Finally, autonomously self-healing conducting graphitic inks have been developed containing $Nd_2Fe_{14}B$ microparticles in a styrene-isoprene-styrene matrix.[134] $Nd_2Fe_{14}B$ microparticles are permanently magnetic and exhibit a strong attraction between themselves. As such, the conductive inks were able to self-heal gaps of up to 3 mm and recover their electrical properties within 50 ms, see Figure 27~~8~~. In addition, the damage could be recovered after multiple healing cycles.[134] These inks have the potential to be used to self-repair electrical contacts in flexible devices as the fragility of printed electronics restricts their current implementation. Due to the autonomous self-healing ability, Bandodkar *et al.* also utilised a polymer composite as a binder for a battery or in wearable electrochemical sensors and demonstrated that both could self-heal autonomously without external stimuli within a second.[134]

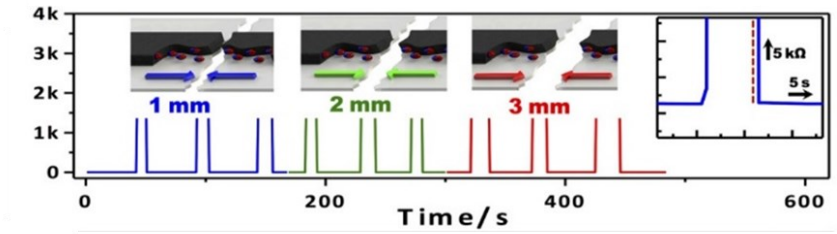

Figure 27~~8~~ Electrical conductivity studies during the self-healing process. The $Nd_2Fe_{14}B$ containing inks were able to recover their electrical properties instantly and autonomously up to a separation gap of 3 mm. Reproduced with permission.[134] American Association for the Advancement of Science, 2016.

4. Combinatorial Environments

The work presented to date has led to an improvement in the robustness of materials through structural design, chemistry and/or manufacturing approaches in order to find utility in specific extreme environments. Further research has been considering a combination of extreme environments.

Liu *et al.* developed a superhydrophilic superoleophobic (3-aminopropyl) triethoxysilane-functionalized silica/polyvinyl alcohol organo-hydrogel along with an oil-water separation mesh.[135] The material possessed the ability to self-heal at temperatures as low as -25 °C, whilst also maintaining integrity after immersion in a variety of solutions for 15 days; these included deionized water, HCl solution (1 M), NaOH solution (1 M), saturated NaCl solution, artificial seawater and saturated NaCl solution (−20 °C). The water/ethylene glycol solvent was responsible for the low-temperature tolerance. The stability in various solutions arose from multi-sized APTES-SiO_2 nanoparticles in the system, exhibiting a multiscale rough surface structure, enabling water to enter gaps to reduce ~~the contact between~~ the surface and oil droplet contact~~s~~. The self-healing primarily occurs through a heating and cooling process whereby crystalline domains and hydrogen bonds dynamically dissociate and associate. This organo-hydrogel has applications in underwater oil transport, wearable oil-repellent or as an oil-water separation material fit for extreme low temperature, underwater and corrosive environments.

Formatted: Font color: Dark Red

Recently, Guo *et al.* reported on a supramolecular elastomer design that incorporated synergistic interactions of multiple dynamic bonds, including disulfide metathesis, strong hydrogen bond crosslinks and weak hydrogen bond crosslinks, into a polydimethylsiloxane backbone.[8] These synergistic effects enabled the elastomer to self-heal in extreme low temperature (-40 °C), super cooled saltwater (30% NaCl solution at -10 °C), in strong acid/alkali conditions (pH = 0 or 14) and could be integrated with gallium indium (liquid metal) alloy for self-healing as an artificial conductor. The disulfide metathesis was influential in the self-healing process, where the strong hydrogen bonding crosslinks had the greatest effect on the stretchability and mechanical strength, and the weak hydrogen bonding crosslinks allowed for energy dissipation. As expected, tailoring the balance between these interactions led to profound changes in the mechanical properties, such as the stretchability increasing by an order of magnitude. With regard to self-healing efficiency, samples could reach up to 93% healing

with respect to tensile strain at ambient temperature for 2 hours. This efficiency was also achieved after immersion in water for 24 hours. During immersion in 30% NaCl solution at -10 °C, 24 hours of immersion achieved 89% efficiency. Similar efficiencies were achieved in very high and low *pH* conditions (*pH* = 0 and 14). At -40 °C, the efficiency reached above 52% and had 86% at 4 °C. The high self-healing efficiencies were due to the viscous and fluid-like properties of the material, from its low T_g (< -50 °C). Additional advantages of this material are that there is no significant surface ageing and healing processes can be repeated. Due to the breadth of self-healing in extreme environments, the range of applications is large, from electronic communication devices in marine or polar environments, to flexible electronic skin devices and to electrical conductors. This material is of interest for extreme low temperature, underwater, corrosive and electrical environments. The relatively small number of materials developed for healing under a combination of extreme conditions indicate that this is an area of research worthy of further investigation and materials development.

5. Summary and outlook

Self-healing polymers have the potential for effective operation within extreme environments. Such polymers can limit the need for human intervention in order to repair components and devices within these environments, which can be potentially high risk or threating to life. In addition, their use can reduce the cost of expensive repairs for inaccessible or remote components, prolong their service life, and maintaining their operational performance. In challenging environments, extrinsic self-healing methods that use microcapsule-loaded healing agents in a polymer matrix have wide applicability and show good self-healing efficiencies; however, this approach is irreversible and limited to a single healing operation. Extrinsic microvascular networks allow multiple self-healing events, however, their fabrication can be difficult, time consuming and expensive. In comparison, intrinsic self-healing in extreme

environments relies on the macromolecular design of polymer structures. High self-healing efficiencies and, theoretically, an infinite number of self-healing cycles can be achieved through dynamic covalent bonds or non-covalent interactions. This latter approach offers versatile opportunities for a smart and truly biomimetic design.

Over the last 25 years, advances in synthetic polymer chemistry and the development of reversible deactivation radical polymerisation (RDRP) methods have provided unprecedented control over the molecular weight, composition, architecture, and functionality of polymeric materials. However, to date there have been limited reports where these techniques have been used in the development of polymers that can function and self-heal in extreme environments. Future work in this area should focus on using the synthetic control offered by RDRP techniques, such as reversible addition-fragmentation chain-transfer (RAFT) polymerisation and atom transfer radical polymerisation (ATRP), to design polymers that have the functionality for dynamic bonding evenly distributed through each polymer chain, or that are confined in single blocks,[136] or the terminal groups of large dendritic structures. These techniques offer the potential to build on and optimise the results achieved through the functionalisation of commercial materials to enable mass manufacture and low-cost processing of self-healing polymers.

Each extreme environment presents a specific technical challenge which must be overcome within the polymer design for successful and efficient self-healing to take place. For example, the low temperature environment represents kinetic challenges for the rate of the reaction. In extreme environments such as the deep ocean there is an additional challenge of requiring self-healing mechanisms that are not disrupted by the presence of water molecules, high salinity, or high-pressure. Due to the limited investigations on self-healing materials for extreme environments, many pathways remain unexplored for each environment, and there are

opportunities for the development of new structures and chemistries that allow for the range of current, and well understood, healing mechanisms to be extended into extreme environments. In addition to the self-healing mechanism, the physical, thermal and viscoelastic properties of the polymer must be carefully considered for each different extreme environment. For example, to achieve healing in a high intensity UV light environment, polymer chains need to be designed which are also resilient to photo-induced chain scission. Therefore, for each extreme environment presented, careful consideration of the responsiveness of polymer chains needs to be considered. Nevertheless, there are also opportunities to take advantage of the unique conditions of each extreme environment to create new self-healing mechanisms; this can include exploiting the thermal energy associated with high temperature operation, the presence of high energy UV light and high electrical/magnetic fields. In terms of self-healing under a magnetic field, approaches to date have focussed on the *Néel relaxation* of fillers, and there is currently no intrinsic self-healing approach that utilises the magnetic field to stimulate self-healing.

With regards to commercialision, there is a need for transfer academic research to industry. This can be facilitated by the creation of higher technology readiness (TRL) prototypes that demonstrate structures or devices that self-heal in extreme environments to highlight the potential of the technology, for example in aircraft skins or marine structures. Selection of the dynamic chemistry for healing and synthesis method also needs to be able to supply materials at large scale; for example for self healing corrosion resistant coatings on marine structures.

Finally, future attractive applications lie in the fields of wireless sensors,[137] self-powered sensors,[138] energy generators and soft robotics, which are self-powered and can operate in remote locations such as the ocean, oil fields, and space. Multifunctional and self-healing polymer based nanocomposites are suitable candidates due to their unique characteristics, such as their lightweight, ease of manufacturing and modification, versatility, and low cost. The

combination of intrinsic and extrinsic approaches in polymer composites and nanocomposites will further expand their self-healing capacity for the development of energy generators and self-powered sensors for soft machines in low pressure, low temperature and intense UV light operation. The technical challenges associated with self-healing in extreme environments provides exciting opportunities for the development of new polymer chemistries and new healing mechanisms to transition into real-world applications.

Aknowledgement

MP thanks the support from The Leverhulme Trust for the Leverhulme Research Fellowship RF-2020-503\4.

Table1 Self-healing polymers and composites under extreme conditions

Polymers	**Healing Mechanism**	**Healing Conditions**	**Mechanical Properties**	**Electrical Properties**	**Healing Efficiency %**	**Preparation methods**	Applications
Low Temperature							
P-carboxylic-acid-methylester-picolinazide & phenylacetylene[33]	Copper-catalysed azide/alkyne "click" reaction enables crosslinking of three-arm star polymers	Cold healing 10 °C			-	Star-shaped azido-telechelic poly(isobutylene) synthesised from 2-(6-azidomethyl)-pyridine-4-carboxylic acid refluxed with oxalyl chloride, followed by additions of star-shaped PIB-OH and 4-(dimethlyaminopropyl)-N'-ethylcarbodiimide hydrochloride.	Low Temperature
2-(dimethylamino)ethyl methacrylate, glyceryl monomethacrylate and butyl methacrylate cross-linked with hexamethylene diisocyanate[41]	Swelling below lower critical solution temperature and metal-ligand coordination	Cold healing 5 °C and pH ~ 4	Tensile strength, 5.2 MPa		~ 100	2-(dimethylamino)ethyl methacrylate, glyceryl monomethacrylate and butyl methacrylate monomers underwent free-radical polymerization with subsequent cross-linking with hexamethylene diisocyanate.	Low Temperature & low pH Material coating
Linear polydimethylsiloxane cross-linked with an Fe(III)-2,6-pyridinedicarboxamide coordination complex[34]	Metal-ligand coordination	Cold-healing -20 °C	Maximum fracture strain, 4500%	Dielectric constant, 6.4 Dielectric strength, 18.8 MVm^{-1}	~ 68	PDMS oligomer that contained 2,6-pyidinedicarboxamide was prepared by condensation reaction between bis(3-aminopropyl)-terminated poly(dimethylsiloxane) and 2,6-pyridinedicarbonyl dichloride.	Low Temperature Artificial muscle actuators
Poly(ethylene-co-methacrylic acid)[39]	Hydrogen bonding	Ballistic puncture -50 °C to 110 °C	Tensile Strength, ~40 MPa Strain, ~1100%		-	Poly(ethylene-co-methacrylic acid) pelletized resins were dried under vacuum prior to moulding. Films were produced through compression moulding.	Low Temperature Combat aircraft fuel tanks and protective barrier in oil tankers.
Silanol-terminated polydimethylsiloxanes	Dynamic boron cross-linking reaction and flexible	Cold crack healing -25 °C	T_g, -110 °C		>80	Series of PDMS-OH and trimethoxyboroxine stirred in oil bath prior to addition of isophorone	Fatigue loading & Low Temperature

and trimethoxyboroxine[42]	polymer chain diffusion at the fracture interface		Tensile Strength, 8.4 MPa			diisocyanurate to obtain intermediate product. Mixture was dried in oven.	
Glass fibre-reinforced laminate embedded with wave-like hollow vessels and conductive sheets[32]	Conductive layer providing heat to defrost internally. Healing agent: RT151 two-part epoxy	Internal defrosting -60 °C	Tensile Strength, 60 MPa	Electrical Conductivity, 70,000 S m^{-1}	~100	Hollow vessels made by vaporization of sacrificial components and resin infusion used to make fibre reinforced composites.	Low Temperature Aircraft, satellites and wind turbines.
Commercial enamel paint[30]	Conversion of silanol groups to viscoelastic product Healing agent :Silanol-terminated polydimethylsiloxane	Crack Healing -20 °C			~80 ~~(?)~~	Silanol-terminated polydimethylsiloxane and dibutyltin dilaurate were microencapsulated using urea-formaldehyde polymer and polyurethane as shell materials, respectively.	Low Temperature Enamel paint coating
Diglycidyl ether of bisphenol A and diglycidyl tetrahydro-o-phthalate epoxy resins with mercaptan hardener[37]	Hydrogen bonding (?)	Cold crack-healing -10 °C	Tensile Strength, >40 MPa		86	Diglycidyl tetrahydro-o-phthalate was stirred with sodium styrene-maleate copolymer and subsequently agitated with a mixture of formaldehyde and the prepolymer of melamine.	Low Temperature Epoxy Resin Adhesive
Sodium methacrylate & [2-(methacryloyloxy)-ethyl] trimethyl ammonium chloride[35]	Hydrogen bonding	Cold Healing -20 °C	Tensile Strength, ~0.01 MPa Strain, >7000%		85	Gels prepared from mixtures of the monomers with glycerol and water. Cross-linked with N,N'-bis(acryloyl) cystamine and mixed with N,N,N',N'-tetramethylethylenediamine.	Low Temperature Motion sensing wearable devices and signal transition material
High Temperature							
9-anthracenemethanol & N-(2-hydroxyethyl)-maleimide[16]	Diels-Alder	Thermal healing 140 °C	Tensile Strength, 89.4 MPa T_g , 64.1 °C		94	N-(2-hydroxyethyl)-maleimide synthesised from maleic anhydride and furan. Subsequently refluxed with 9-anthracenemethanol in toluene.	High Temperature Structural Applications
Isocyanurate-oxazolidone[21]	Transformation of isocyanurate with epoxide	Thermal healing 200 °C	Tensile Strength, 93 MPa		85	Toluene-2,4-diisocyanate, N,N-dimethylbenzylamine and diglycidyl ether of bisphenol F were mixed.	High Temperature

	groups yielding new oxazolidone rings		T_g, 285 °C			Unidirectional carbon fabric layered up followed by vacuum assisted transfer moulding.	CFRP composite panels
Epoxidized Natural Rubber / Citric acid-modified bentonite composite[139]	Transesterification reactions of β-hydroxyl ester linkages	Thermal healing 150 °C	Tensile Strength, 9.5 MPa		>90	Epoxidized Natural Rubber masticated with 0-30 wt% of CA-modified bentonite on a 2-roll mill, then subjected to compression moulding.	High Temperature
CY 179 epoxy resin[29]	Cationic chain polymerization with healing agent Trifluoromethanesulfonic acid	Ambient Crack Healing			79	Trifluoromethanesulfonic acid infiltrated into silica walled hollow microcapsules.	High Temperature Epoxy resin
N-(2-hydroxyethyl)-maleimide & 3-(N, N-Bis (2-hydroxyethyl) amine) propionic acid-9-anthracenemethanol ester[20]	Diels-Alder	Thermal Healing 90 °C	Tensile Strength, 10.7 MPa Strain, 662% T_g, 16 °C		91	N-(2-hydroxyethyl)-maleimide synthesised from maleic anhydride and furan. Subsequently reacted with 3-(N, N-Bis (2-hydroxyethyl) amine) propionic acid-9-anthracenemethanol ester and a range of solvents to form the linear polyurethanes with pendant anthryl groups.	High Temperature Smart materials
1,1-(methylene-di-1,4-phenylene)bismaleide-furfuryl glycidyl ether-J4000[23]	Diels-Alder	Thermal Healing 80 °C	Tensile Strength, >2 MPa Strain, >400% T_g, -48 °C		98	Furfuryl glycidyl ether stirred and reacted with a Jeffamine for 7 days, prior to mixing with 1,1-(methylene-di-1,4-phenylene)bismaleide.	High Temperature Soft pneumatic robots
1,1-(methylene-di-1,4-phenylene)bismaleide-furfuryl glycidyl ether-J400[26]	Diels-Alder	Thermal Healing 120 °C	Tensile Strength, 17 MPa Strain, 1% T_g, 74 °C		~100	Furfuryl glycidyl ether stirred and reacted with a Jeffamine for 7 days, prior to mixing with 1,1-(methylene-di-1,4-phenylene)bismaleide. Further implemented into the mechanical fuse.	High Temperature Sacrificial self-healing fuse for robotic systems
Polycaprolactone dimethacrylate with methacrylates bearing 2-ureido-	Reversible formation of four cooperative hydrogen bonds between two UPy units	Thermal healing at 80 °C	Tensile Strength, 13 MPa		53	To print, a mixture of PCLDMA and UPyMA containing 4 wt% of 2,4,6-trimethylbenzoyl-diphenyl-	High Temperature 4D Printing

4[1H]-pyrimidinone motifs[27]			Strain, 300%			phosphinoxide as photoinitiator and chloroform was used. The formulation was kept at 45 °C during the printing process by a custom made hot plate.	
[4-6% (mercaptopropyl)methylsiloxane]-dimethylsiloxane with vinyl-terminated polydimethylsiloxanes[28]	Disulfide bond methathesis	Thermal healing 60 °C	Tensile strength, 16 KPa		~100	[4-6% (mercaptopropyl)methylsiloxane]-dimethylsiloxane was first oxidized with iodobenzene diacetate to form a thiol-disulfide oligomer. The oligomer then undergoes a photoinitiated thiol-ene reaction with vinyl-terminated polydimethylsiloxanes to form a solid elastomer.	High Temperature 3D soft actuator
1,1-(methylene-di-1,4-phenylene)bismaleide-furfuryl glycidyl ether-JT5000 and furan-maleimide[10]	Diels-Alder	Thermal Healing 90 °C	Tensile Strength, 1.6 MPa Strain, 131%		95	Furfuryl glycidyl ether reacts with a Jeffamine. This furan-functionalized Jeffamine is afterward mixed with 1,1-(methylene-di-1,4-phenylene)bismaleide and subsequently dissolved in chloroform.	High Temperature 3D soft actuator
Fatigue							
Ethyl phenylacetate solvent and diglycidyl ether of bisphenol A epoxy[48]	Damage ruptures microcapsules, healing agents temporarily swell the epoxy matrix and rebonds the crack	Ambient crack healing	Number of transverse cracks saturates 10,550 ± 2,610 cycles		52.8	Polyurethane/poly(urea-formaldehyde) microcapsules manufacture by in-situ polymerization. Core material was a mixture of EPON 862 resin and EPA solvent. Cross-ply laminated composites manufactured from prepreg. Composite panels cured by hot pressing with vacuum bagging.	Fatigue loads
Underwater							
Poly(vinylidene fluoride-co-hexafluoropropylene), vinylidene fluoride and hexafluoropropylene[52]	Dipole-dipole interactions between hydrophobic C-F bonds	Ambient Crack Healing and Underwater pH = 1 & 13	Tensile Strength, ~1 MPa Strain, 1060% T_g, -35.5 °C		~22	Poly(vinylidene fluoride-co-hexafluoropropylene) and dibutyl phthalate were dissolved in anhydrous acetone and were mixed and evaporated at room temperature in a petri dish prior to compression moulding.	Underwater & low/high pH

Catechol-functionalized polymers with p-phenyldiboronic acid[54]	Absorbed water enhances esterification between catechol and boronic acid moieties, shifts equilibrium towards hydrolysis and exposes free groups on surface	Marginal swelling in seawater	Tensile Strength, 2.8 MPa T_g, -11.8 °C		91	To a nitrogen-purged Schlenk flask, dopamine acylamide, dimethyl 2,2'-azobis(2-methylpropionate), n-butyl acrylate and anhydrous ethanol was mixed. Solution was subsequently degassed via three freeze-pump-thaw cycles and backfilled with nitrogen, prior to being stirred in an oil bath.	Underwater
Hyperbranched polyurethane-mercaptosuccinic acid-acrylonitrile butadiene styrene[50]	Hydrogen Bonding, Hydrophobic Interactions and eventual Rearrangement/Randomization of the networks of the hyperbranched polymer	Acidic Water pH = 4	Tensile Strength, ~2 MPa Strain, 2000%		87	PTMEG was dissolved in DMF and the DMF solution of IPDI was incorporated under nitrogen. Prepolymerization proceeded under mechanical agitation. ~~The~~ DMF solutions of HBPE, MSA, 1,3-propanedithiol and ABS were added in stages with a UV irradiation procedure after the final addition.	Underwater & low pH Sealing elements, flexible hosepipes and linings.
Adamantane glycol diglycidyl and etherethylenediamine-β-cyclodextrin with graphene oxide nanosheets[55]	Dynamic host-guest interactions between cyclodextrin on the graphene surface and adamantane on the polymer chains.	Immersion in 3.5 wt% NaCl solution			-	1-adamantanecarboxylic acid and glycol diglycidyl ether dissolved in toluene successively, prior to triphelyphosphine addition and refluxing. β-cyclodextrin was mixed with prior formulation to form the graphene-epoxy nanocomposites.	Underwater Anticorrosion coatings.
Corrosion							
Polyaniline shell and sodium alginate core microcapsule structure[140]	Damage ruptures microcapsule, sodium alginate outflows and reacts with Ca^{2+} in the defect region forming a gel structure preventing corrosion.	Ambient crack healing	Tensile Strength, 86.8 MPa	R_p, 1207 kΩ cm^2	90	Aniline and DMF were stirred and eventually had ammonium persulfate, dissolved in HCl, added dropwise to it before being diluted in water and passed through membrane. This was then added into a PANI-NMP solution.	Corrosion protection of water-delivery pipelines
Poly(borosiloxane)[141]	Reptile motion	Crack Healing	T_g, -5 °C	Bode impedance, 6.5 log (Z Ohm^{-1})	-	Polymer film was coated over the metal (Ti) by the drop-casting method and dried thoroughly.	Metal c~~C~~orrosion Protectant

				Corrosion Current, -4.3 mA Corrosion Potential, -0.54 V Passive Current Density, -1.5			
Vacuum							
Reactive mixture containing trimethylolpropane triallyl ether and ethylene glycol dimercaptopropionate with tributylborane catalyst[79]	Oxygen driven polymerisation of reactive mixture	Presence of oxygen	-	-	Solid plug formed within seconds of bullet penetration test	Tributylborane initiated the thiol-ene reaction of the reactive mixture upon oxygen exposure	Protective aerospace structures – under vacuum
Gelator and polymerisation based microcapsule and microvascular system in epoxy resin [84]	Initial gelation caused by bis-acylhydrazine-terminated poly(ethylene glycol) and tris[(4-formylphenoxy) methyl]ethane. Polymerisation between 2-hydroxyethyl methacrylate and 2-hydroxyethyl acrylate	Catalytic controlled gelation and polymerisation	Impact testing, 1.2 kN	-	100% sealing and 100% impact recovery efficiency	Microcapsules containing both gelation and polymerisation components were mixed into epoxy resin and cured for up to 2 days	Sealing and recovery of structures under vacuum
Epoxy based healing utilising poly(ethylenimine) as a curing agent [81]	Epoxy curing upon exposure to oxygen	Presence of oxygen	-	-	Puncture testing of vacuum insulation panels	Mixing of epoxy Epon 8111 with poly(ethylenimine) in a vacuum insulation panel	Vacuum insulation panels
2-ureido-4[1H]-pyrimidinone (UPy)-functionalized polyhedral oligomeric	Reversible quadruple hydrogen bonding between UPy chains	Thermal (or solar under a low earth	-	-	Optical imaging	2-(6-Isocyanato-hexylaminocarbonylamino)-6-methyl-4-[1H]-pyrimidinone, octa-hydroxylated POSS and dibutyltin dilaurate were	Atomic oxygen resistant coatings

silsesquioxane (POSS) polymeric coatings[88]		orbit) heating 80 ºC			Visual SEM inspection of coating surface	dissolved in chloroform and mixed for 7 days, prior to being washed with chloroform for 14 days in a Soxhlet extractor. Followed by hot pressing of the coatings onto Kapton sheets	Solar arrays and optical devices on spacecraft
UV Radiation							
Diglycidylether of bisphenol A (DEGBA) cross-linked with *m*-xylylenediamine (MXDA) and 4-(heptadecafluorooctyl)aniline HFOA)[93]	UV radiation for photothermal effect – promotion of chain diffusion and chain reentanglement.	UV light from solar simulator	-	-	99% (optical imaging analysis)	HFOA, MXDA, aniline black and DEGBA mixed at 100 °C with N,N-dimethylformamide solvent. Spin coated then thermally cured.	Outdoor epoxy coatings
Oxolane-chitosan-poly(urethane) (OXO-CHI-PUR) network[142]	UV light driven free radical catalysed poly(urea) to poly(urethane), formation of linear –C-O-C- from ring opened OXO and chair to boat conformational change in glycosine units of CHI	302 nm fluorescent lamp (120 W)	-	-	-	OXO-CHI was sonicated for 12 hours then stirred at 80 ° for 48 hours in DMSO. Hexamethylene diisocyanate added under nitrogen as well as poly(ethylene glycol) and dibutyltin dilaurate and stirred for 10 minutes.	Self-healing poly(urethanes)
Coumarin based poly(urethane)[97]	UV light driven dimerization of coumarin followed by thermal heating to crosslinking poly(urethane) with coumarin dimers	254 nm and 365 nm UV light (14.4 mW cm^{-2})	Tensile strength, 14.4 MPa	-	92.5% tensile strength recovery	Poly(urethane) and coumarin were dissolved in N,N-dimethylformamide and mixed together and cured	Electronic skin, electrochemical sensors, coatings
Diglycidyl ether of bisphenol A (DEGBA) and furfurylamine with MXene flakes[143]	UV radiation for photothermal effect – to break and reform diels alder crosslinking	Near infrared light and solar light	Pencil hardness 4h-5H (from B-HB)	-	Visual observation	DEGBA and furfurylamine was dissolved in N,N-dimethylformamide stirred at 100 °C. MXene added to solution and dispersed by sonication and stirring. Sample spin coated and cured at 60 °C.	Epoxy coatings
Epoxidised soybean oil (ESO) cross-linked by citric acid with gold nanoparticles[144]	Light radiation for photothermal effect – molecular rearrangements from transesterification of β-hydroxyester groups from heating of gold nanoparticles	Green laser (700 mW)	Tensile strength, 1.2 MPa	-	90-100%	ESO, gold nanoparticles and citric acid stirred in water at 90 °C. Solvent cast and cured at various temperatures up to 160 °C.	Self-healing bio-based polymers

Cross-linked poly(ethylene oxide) (PEO) with poly(ethylene glycol) (PEG) doped gold nanoparticles[99]	Light radiation for photothermal effect – crystal melting and recrystallization from heating of gold nanoparticles	532 nm laser (1 W)	Tensile strength, 8 MPa	-	62%	PEG functionalised gold nanoparticles and acrylate terminated PEO were mixed together in water and sonicated. Crosslinking was initiated by N,N,N',N'-tetramethylethylenediamine	Combined shape memory and self-healing polymers
Poly(dimethylsiloxane) and poly(urethane) cross-linked networks containing cooper chloride catalyst[145]	UV light radiation reaction – Cu-O undergoes tetrahedral to distorted tetrahedral transition leading to a low energy charge transfer to facilitate Si-O-Si cleavage and reformation	302 nm fluorescent UV lamp (15 W)	Young's modulus, 0.92 MPa	-	92%	Poly(dimethylsiloxane), hexamethylene diisocyanate and copper chloride were stirred in N,N-dimethylformamide under an N_2 atmosphere and cured at 75 °C for 72 hrs	Light stimulated self-healing polymers
Diglycidyl ether of bisphenol A and epoxidised hydrogenated bisphenol A epoxy resin with SiO_2 containing microcapsules[90]	UV-light initiated cationic polymerisation to crosslink the epoxy chains together in the damaged region	365 nm UV lamp (1.2 mW cm^{-2})	-	-	89% curing efficiency	SiO_2 microcapsules prepared by oil in water emulsion of diglycidyl ether of bisphenol A, epoxidised hydrogenated bisphenol A, propylene carbonate and tetraethyl orthosilicate into poly(ethyleneoxide-*b*-propylene oxide-*b*-ethylene oxide). SiO_2 microcapsules mixed into epoxy resin and cured at 24 hrs.	Aerospace coatings
Epoxidised soybean oil microcapsules in epoxy resin[146]	Sunlight/xenon light irradiation promoting silyl radical cationic polymerisation	320 nm xenon lamp or sunlight (24-31 mW cm^{-2})	-	-	70% curing efficiency	Epoxidised soybean oil microcapsules were prepared using an oil in water emulsion preparation. Microcapsules were mixed at room temperature and cured for 2 days.	Long term, environmentally resistant epoxy coatings
Diglycidyl ether of bisphenol A epoxy resin with poly(urea-formaldehyde)/TiO_2 microcapsules containing photosensitive resin[92]	UV light stimulated photoreaction between epoxy resin and photosensitive resin	UV light	-	8.2 μA at 3 V	90% curing efficiency. Electrical current recovered to 0.11 mA	The prepared photosensitive resin containing microcapsules were mixed into the epoxy resin and cured for 48 hrs.	Long term epoxy coatings
Thermoplastic poly(urethane) with poly(p-phenylene	UV radiation for photothermal effect –	Xenon lamp (500 W)	Tensile strength, 5.5 GPa		82.5 % self-healing	PBO fibres were modified with poly(dopamine). Ag was immobilised using 3 minute microwave procedure and	High performance light triggered

benzobisoxazole) (PBO) fibres with immobilised Ag-Cu_2S particles[147]	reduces viscosity for diffusion of polymer matrix		Interfacial shear strength, 70 MPa		recovery based interfacial shear strength	Cu_2S was deposited using a hydrothermal procedure. Modified PBO fibres were dispersed into poly(urethane).	self-healing composites
Fabricated skin on copper-clad polyimide substrate sheets using polyimide sheets and an ultraviolet-curable epoxy[98]	Ambient light cures flowable epoxy	Ambient light				The self-healing skin design employs Kapton® layers clad with copper. Loctite Impruv 365 UV-curable epoxy was selected for skin assembly. A polyethylene terephthalate film was used to expose dot arrays of the UV-curable epoxy to create columns. A passive, wireless telemetry scheme is integrated with the skin concept to detect skin damage and identify its location.	Self-healing skin sensors
Diels-Alder based polyurethane covalently linked with functionalized graphene nanosheets[101]	IR radiation enables reversible Diels-Alder mechanisms	Infrared laser irradiation (980 nm)	Tensile strength, 36 MPa Strain, 1100%	Volume resistivity, 5.6×10^{11} Ω·cm	96	Furfuryl alcohol and bismaleimide were mixed in DMF prior to addition of the functionalized graphene nanosheets. The resulting mixtures were pressed in toTeflon plates and dried to fabricate the films.	Intelligent flexible electronics
Poly(N-isopropylacrylamide) with poly(N,N-dimethylacrylamide)[102]	IR radiation enables healing of non-covalent bonds between clay plates and polymer amide groups	Infrared laser irradiation (980 nm)	Tensile strength, 0.13 MPa Strain, 400%		-	Graphene oxide-based PDMAA and PNIPAM NC hydrogel were synthesised separately by in situ free radical polymerization.	Soft actuation Flowing control Biomimetic devices
Metallopolymers based on zinc(II)–terpyridine coordination nodes bearing photoisomerizable diazobenzene units[103]	Metal-ligand coordination interactions	UV light			-	Ligands were dissolved in chloroform under an argon atmosphere prior to addition of Zn(BF4)2 in MeOH. The solution was stirred for 12 hours.	Soft actuation
Anisotropic hydrogels of	IR stimulated dynamic thiolate-metal coordination interactions	Infrared laser irradiation (808 nm)	Tensile strength, 3 MPa		85	N,Nbis(acryloyl)cystamine was added into Ag	Robotic actuation

metal nanostructure assembly lamellae with thiolate-modified metal assemblies as multifunctional crosslinkers[104]		Acid solution (1 mol L^{-1})	Strain, 2500%			NPs solution, followed by ultra-sonication. Followed by addition of acrylamide as monomer and Irgacure 2959 before irradiation under UV light to prepare hydrogel.	
Electric Field							
Dispersion of dicyclopentadiene filled urea-formaldehyde microcapsules in epoxy resin[106]	Healing agent reacting with catalyst to produce a polymer, which fills the microcracks from electrical treeing	Room temperature	-	-	-	Acid-catalysed in situ polymerisation in an oil-in-water emulsion	Rigid, high electric field environments
Naturally derived 'drying oil' from alyk benzene fluid and tung oil[112]	Drying oil reacted upon exposure to air to heal failure site	Room temperature	-	Electrical breakdown strength, 85 kV m^{-1}	-	Mixed together	Fluid filled cables
Composite based on 20 wt% reduced graphite nanoplatelets in silicone[115]	Sparks partially burn electrode and dielectric film, silicone is oxidized to silica, due to high oxygen presence, and turns that part of the electrode inactive.	Electric Field	Tensile strength, ~0.35 MPa Strain, ~175%	Electrical Conductivity, 0.35 S cm^{-1} at 0% strain Sheet Resistance, 0.1 kΩ sq^{-1} Electrical Breakdown Voltage, 2.4 kV	-	Homogeneous composites containing reduced graphene nanoplatelets were prepared in a solution of PDMS:Neukasil A7 in toluene by sonication in a bath, followed by passing the composite several times through a three roll mill.	Electrode for Actuators
Liquid metal electrodes with in-plane self-healing capability for dielectric elastomer actuators[116]	Two-dimensional in-plane self-healing. I) A capacitor is created between two charged boundaries, where charges converge and the distance is shorter and the attraction force is greater,	Electric Field	Strain, 360%	Electrical Breakdown Voltage, 3.5 kV	-	Liquid metal was directly painted on the 300% biaxially prestrained VHB 4905 film to form compliant electrodes.	Artificial muscle actuation Flexible electronics

	liquid metal breaks its thin oxide layer film and merge. II) Actuation causes expansion of the film, which in turn causes a center-out micro-flow of the liquid metal.						Wearable devices Smart clothing
Two-phase dielectric consisting of an open-cell silicone sponge saturated with silicone oil[117]	Silicone oil flows into voids, reestablishing the dielectric structure	Electric Field		Electrical Breakdown Voltage, 5 kV	-	Fabricated from two flexible circular electrodes made from Nyogel carbon grease embedded in a layer of Platsil Gel 00 Silicone, and a circular silicone sponge made from an open cell silicone foam.	Actuation
Hydraulically amplified self-healing electrostatic (HASEL) actuators[118]	Liquid dielectrics immediately return to an insulating state after breakdown	Electric Field		Electrical Breakdown Voltage, 29 kV	-	An elastomeric shell is partially covered by a pair of opposing electrodes and filled with a liquid dielectric	Soft robotic actuation
Methyl thioglycolate-modified styrene-butadiene-styrene[128]	Intermolecular electrostatic interactions taking place between the methyl thioglycolate–modified butadiene block and the styrene block of SBS	Electric Field	Strain, 569%	Breakdown Strength, 30 kV mm^{-1} Dielectric Constant, 11.4	67	The styrene-butadiene-styrene block copolymer was dissolved in tetrahydrofuran. Then 2-dimethoxy-2-phenylacetophenone and methyl thioglycolate were added to the solution, followed by irradiating with UV light (365 nm). After purification by precipitation in hexane, sample was dried in a vacuum oven at 60 °C overnight.	Soft robotic actuation Energy harvesting devices
Magnetic Field							
Silicone polymer with 2-ureido-4[1H]-pyrimidone (UPy) and Fe_3O_4 particles[128]	Magnetically induced heating of polymer	MagneTherm alternating magnetic frequency (110.1 kHz, 250 Oe)	Tensile Strength, 13 kPa Strain, 37%	-	70% tensile strength recovery, 78% strain at break recovery	Solvent casted composite using THF and DMF, and sonication of Fe_3O_4 for dispersion	Soft elastomer applications
Styrene-isoprene-styrene based graphitic inks containing	Magnetic attraction induced self-healing	Autonomous	-	0.3 mA current (at 0.2 V)	Recovers to 0.3 mA	Solvent mixing in xylene	Conducting inks, electrodes and batteries

Formatted: Font: 10 pt, Not Italic

$Nd_2Fe_{14}B$ microparticles[134]					current (at 0.2 V)		
Thermoplastic poly(ethylene vinyl acetate) with $Mn_xZn_{1-x}Fe_2O_4$ nanoparticles[125]	Magnetically induced heating of polymer	Alternating magnetic frequency (up to 10 kOe)	-	-	Notch test – 100% recovery	Solvent mixing followed by solvent casting approach	Wire insulation materials
Bitumen with added iron oxide nanoparticles[127]	Magnetically induced heating of material	Alternating magnetic frequency	-	-	Visual recovery	Solvent mixing approach	Crack repairing roads and pavements
Poly(ethylene-co-vinyl acetate) with $Mn_{0.8-}Zn_{0.2}Fe_2O_4$ nanoparticles[132]	Magnetic field induces shape memory effect followed by chain entanglement	Alternating magnetic frequency	Maximum load, 16N Maximum extension, 120 mm	-	> 95%	Solvent mixing followed by solvent casting approach	Reusable biomedical devices e.g. coated guidewires
Magnetite containing bitumen composites[131]	Magnetically induced heating of material	Alternating magnetic frequency (380 kHz)	-	-	Followed temperature changes and visual recovery	Melt mixing	Crack repairing roads and pavements
Polystyrene nanocomposites filled with nanoparticles with a cobalt iron oxide core and a manganese iron oxide shell[124]	Magnetically induced heating of polymer	Alternating magnetic frequency (244 kHz)	-	-	Visual recovery	Solvent mixing approach	High performance polymer composites
Surface functionalised poly(ethylene glycol) superparamagnetic iron oxide nanoparticles into polypropylene[130]	Magnetically induced heating of polymer	Oscillating magnetic field (968 kHz)	Maximum load, 450 N Maximum extension, 15mm	Breakdown voltage, 13.8 kV. Leakage current, 5 pA.	Load recovery, 100 % Extension recovery, 100 % 100 % breakdown voltage recovery 100 %	Melt mixing	Power cable insulation

					leakage current recovery		
Combinatorial Environments							
Superoleophobic APTES-SiO_2/PVA organohydrogel with oil-water separation mesh[135]	Heating and cooling process whereby crystalline domains and hydrogen bonds dynamically dissociate and reassociate		Tensile Strength, 160 kPa Strain 250% Compressive Strength, 700 kPa Compressive Strain, 99%		Visual recovery	Two differently sized APTES-modified silica nanoparticles were dispersed in mixed solvent (deionized water/ethylene glycol = 1:2 wt/wt) by sonication. PVA was added prior to being poured into a mold placed at −20 °C for 20 min to obtain APTES-SiO2/PVA organohydrogel.	Underwater oil transport Wearable oil-repellent Oil-water separation material
Multi-strength H-bonds and disulfide metathesis in polydimethylsiloxane polymer[8]	Disulfide metathesis, strong hydrogen bond crosslinks and weak hydrogen bond crosslinks	-40 °C Underwater *pH* 0 and 14 Ambient Temperature	Tensile Strength, ~0.1 MPa Strain, ~1500%		93	α, ω-dihydroxyethylpropoxyl-PDMS was reacted with isophorone diisocyanate monomerin N, N′-dimethylacetamide using dibutyltin dilaurate as a catalyst. Then, 4,4′-dithiodianiline (SS) and/or 4,4′-bis(hydroxymethyl)-2,2′-bipyridine (BNB) were added to the solution as a chain extender to complete the PDMS–SS–IP–BNB synthesis.	Electronic communication devices in marine or polar environments Flexible electronic skin devices Electrical conductors

References

[1] F. Gómez, in *Encyclopedia of Astrobiology*, (Eds: M. Gargaud, R. Amils, J. C. Quintanilla, H. J. Cleaves, W. M. Irvine, D. L. Pinti, M. Viso), Springer Berlin Heidelberg, Berlin, Heidelberg 2011, 570.
[2] D. Y. Zhu, M. Z. Rong, M. Q. Zhang, Progress in Polymer Science 2015, 49-50, 175.
[3] B. J. Blaiszik, S. L. B. Kramer, S. C. Olugebefola, J. S. Moore, N. R. Sottos, S. R. White, Annual Review of Materials Research 2010, 40, 179.
[4] J. F. Patrick, B. P. Krull, M. Garg, C. L. Mangun, J. S. Moore, N. R. Sottos, S. R. White, Composites Part A: Applied Science and Manufacturing 2017, 100, 361.
[5] A. M. Wemyss, C. Bowen, C. Plesse, C. Vancaeyzeele, G. T. M. Nguyen, F. Vidal, C. Wan, Materials Science and Engineering: R: Reports 2020, 141, 100561.
[6] J. M. Winne, L. Leibler, F. E. Du Prez, Polymer Chemistry 2019, 10, 6091.
[7] Y. Yang, M. W. Urban, Advanced Materials Interfaces 2018, 5, 1800384.
[8] H. Guo, Y. Han, W. Zhao, J. Yang, L. Zhang, Nature Communications 2020, 11, 2037.
[9] M. Guerre, C. Taplan, J. M. Winne, F. E. Du Prez, Chemical Science 2020, 11, 4855.
[10] E. Roels, S. Terryn, J. Brancart, R. Verhelle, G. Van Assche, B. Vanderborght, Soft Robotics 2020.
[11] P. Rothemund, N. Kellaris, S. K. Mitchell, E. Acome, C. Keplinger, Advanced Materials, n/a, 2003375.
[12] W. Wu, J. Ekeocha, C. Ellingford, S. N. Kurup, C. Wan, in *Self-Healing Polymer-Based Systems*, (Eds: S. Thomas, A. Surendran), Elsevier, 2020, 95.
[13] T. Li, Y. Wang, S. Li, X. Liu, J. Sun, Advanced Materials 2020, 32, 2002706.
[14] Y. Yang, X. Ding, M. W. Urban, Progress in Polymer Science 2015, 49-50, 34.
[15] A. Legrand, C. Soulié-Ziakovic, Macromolecules 2016, 49, 5893.
[16] Y. Heo, M. H. Malakooti, H. A. Sodano, Journal of Materials Chemistry A 2016, 4, 17403.
[17] C. Zeng, H. Seino, J. Ren, K. Hatanaka, N. Yoshie, Polymer 2013, 54, 5351.
[18] N. Yoshie, S. Saito, N. Oya, Polymer 2011, 52, 6074.
[19] L. Zhang, F. Julé, H. A. Sodano, Polymer 2017, 114, 249.
[20] Y. Fang, J. Li, X. Du, Z. Du, X. Cheng, H. Wang, Polymer 2018, 158, 166.
[21] L. Zhang, X. Tian, M. H. Malakooti, H. A. Sodano, Compos. Sci. Technol. 2018, 168, 96.
[22] L. Zhang, J. Lin, H. A. Sodano, J. Appl. Polym. Sci. 2020, 137, 48698.
[23] S. Terryn, J. Brancart, D. Lefeber, G. Van Assche, B. Vanderborght, Science Robotics 2017, 2, eaan4268.
[24] S. Terryn, G. Mathijssen, J. Brancart, D. Lefeber, G. V. Assche, B. Vanderborght, Bioinspiration Biomimetics 2015, 10, 046007.
[25] S. Terryn, J. Brancart, D. Lefeber, G. V. Assche, B. Vanderborght, IEEE Robotics and Automation Letters 2018, 3, 16.
[26] S. Terryn, G. Mathijssen, J. Brancart, T. Verstraten, G. V. Assche, B. Vanderborght, IEEE Transactions on Robotics 2016, 32, 736.
[27] M. Invernizzi, S. Turri, M. Levi, R. Suriano, Eur. Polym. J. 2018, 101, 169.
[28] K. Yu, A. Xin, H. Du, Y. Li, Q. Wang, NPG Asia Materials 2019, 11, 7.
[29] X. J. Ye, Y. X. Song, Y. Zhu, G. C. Yang, M. Z. Rong, M. Q. Zhang, Composites Science and Technology 2014, 104, 40.
[30] D.-M. Kim, Y.-J. Cho, J.-Y. Choi, B.-J. Kim, S.-W. Jin, C.-M. Chung, Materials (Basel, Switzerland) 2017, 10, 1079.
[31] W. H. Binder, *Self-healing polymers*, Wiley Online Library, 2013.
[32] Y. Wang, D. T. Pham, Z. Zhang, J. Li, C. Ji, Y. Liu, J. Leng, 2016, 3, 160488.
[33] S. Neumann, D. Döhler, D. Ströhl, W. H. Binder, Polymer Chemistry 2016, 7, 2342.
[34] C.-H. Li, C. Wang, C. Keplinger, J.-L. Zuo, L. Jin, Y. Sun, P. Zheng, Y. Cao, F. Lissel, C. Linder, X.-Z. You, Z. Bao, Nat. Chem. 2016, 8, 618.

[35] Y. Yang, L. Guan, X. Li, Z. Gao, X. Ren, G. Gao, ACS Applied Materials & Interfaces 2019, 11, 3428.
[36] S. R. White, N. R. Sottos, P. H. Geubelle, J. S. Moore, M. R. Kessler, S. R. Sriram, E. N. Brown, S. Viswanathan, Nature 2001, 409, 794.
[37] Y. C. Yuan, M. Z. Rong, M. Q. Zhang, J. Chen, G. C. Yang, X. M. Li, Macromolecules 2008, 41, 5197.
[38] M. Raimondo, P. Longo, A. Mariconda, L. Guadagno, Advanced Composite Materials 2015, 24, 519.
[39] S. J. Kalista, J. R. Pflug, R. J. Varley, Polymer Chemistry 2013, 4, 4910.
[40] Q. Wang, J. L. Mynar, M. Yoshida, E. Lee, M. Lee, K. Okuro, K. Kinbara, T. Aida, Nature 2010, 463, 339.
[41] S. H. Ju, J. C. Kim, S. M. Noh, I. W. Cheong, Macromolecular Rapid Communications 2018, 39, 1800689.
[42] Y. Deng, X. Liang, X. Pei, K. Zhai, C. Wang, B. Zhang, Y. Bai, Y. Zhang, P. Wang, Y. Tan, K. Xu, Polymer Testing 2019, 76, 43.
[43] F. Mehrabadi, *Experimental and Numerical Failure Analysis of Adhesive Composite Joints*, Vol. 2012, 2012.
[44] V. Kostopoulos, A. Kotrotsos, A. Sousanis, G. Sotiriadis, Composites Science and Technology 2019, 171, 86.
[45] A. S. Jones, J. D. Rule, J. S. Moore, N. R. Sottos, S. R. White, J R Soc Interface 2007, 4, 395.
[46] M. W. Keller, S. R. White, N. R. Sottos, Polymer 2008, 49, 3136.
[47] H. Jin, G. M. Miller, N. R. Sottos, S. R. White, Polymer 2011, 52, 1628.
[48] S. Y. Kim, N. R. Sottos, S. R. White, Composites Science and Technology 2019, 175, 122.
[49] M. Gunasekaran, "Polymer concrete high voltage insulators for the ocean environment", presented at *Proceedings of OCEANS '93*, 18-21 Oct. 1993, 1993.
[50] N. N. Xia, X. M. Xiong, M. Z. Rong, M. Q. Zhang, F. Kong, ACS Applied Materials & Interfaces 2017, 9, 37300.
[51] S. Xu, D. Sheng, X. Liu, F. Ji, Y. Zhou, L. Dong, H. Wu, Y. Yang, Polymer International 2019, 0.
[52] Y. Cao, H. Wu, S. I. Allec, B. M. Wong, D.-S. Nguyen, C. Wang, Advanced Materials 2018, 30, 1804602.
[53] J. Li, H. Ejima, N. Yoshie, ACS Applied Materials & Interfaces 2016, 8, 19047.
[54] C. Kim, H. Ejima, N. Yoshie, RSC Advances 2017, 7, 19288.
[55] C. Liu, J. Li, Z. Jin, P. Hou, H. Zhao, L. Wang, Composites Communications 2019, 15, 155.
[56] T. Matsuda, K. B. Kashi, K. Fushimi, V. J. Gelling, Corros. Sci. 2019, 148, 188.
[57] S. B. Ulaeto, R. Rajan, J. K. Pancrecious, T. Rajan, B. Pai, Progress in Organic Coatings 2017, 111, 294.
[58] M. Samadzadeh, S. H. Boura, M. Peikari, S. Kasiriha, A. Ashrafi, Progress in Organic Coatings 2010, 68, 159; H. Pulikkalparambil, S. Siengchin, J. Parameswaranpillai, Nano-structures & nano-objects 2018, 16, 381; J. P. Wang, X. Song, J. K. Wang, X. Cui, Q. Zhou, T. Qi, G. L. Li, Advanced Materials Interfaces 2019, 6, 1900055.
[59] F. Zhang, P. Ju, M. Pan, D. Zhang, Y. Huang, G. Li, X. Li, Corrosion Science 2018, 144, 74.
[60] B. Rani, B. B. J. Basu, International Journal of corrosion 2012, 2012.
[61] F. Zhang, L. Zhao, H. Chen, S. Xu, D. G. Evans, X. Duan, Angewandte Chemie International Edition 2008, 47, 2466.
[62] M. L. Zheludkevich, D. G. Shchukin, K. A. Yasakau, H. Möhwald, M. G. Ferreira, Chemistry of Materials 2007, 19, 402.
[63] D. G. Shchukin, S. V. Lamaka, K. A. Yasakau, M. L. Zheludkevich, M. G. S. Ferreira, H. Möhwald, The Journal of Physical Chemistry C 2008, 112, 958.
[64] Y. M. Lvov, D. G. Shchukin, H. Möhwald, R. R. Price, ACS Nano 2008, 2, 814.
[65] A. Khan, A. Hassanein, S. Habib, M. Nawaz, R. A. Shakoor, R. Kahraman, ACS Applied Materials & Interfaces 2020, 12, 37571.

[66] E. Shchukina, D. Grigoriev, T. Sviridova, D. Shchukin, Progress in Organic Coatings 2017, 108, 84.
[67] N. Asadi, R. Naderi, M. Mahdavian, Progress in Organic Coatings 2019, 127, 375.
[68] N. Asadi, R. Naderi, M. Mahdavian, Progress in Organic Coatings 2019, 132, 29.
[69] Z. Zheng, M. Schenderlein, X. Huang, N. J. Brownbill, F. Blanc, D. Shchukin, ACS Applied Materials & Interfaces 2015, 7, 22756.
[70] T. Matsuda, N. Jadhav, K. B. Kashi, M. Jensen, A. Suryawanshi, V. J. Gelling, Prog. Org. Coat. 2016, 90, 425.
[71] H.-C. Yu, Y.-T. Zhang, M.-J. Wang, C.-C. Li, Langmuir 2019, 35, 7871.
[72] A. T. O. Lim, C. Cui, H. D. Jang, J. Huang, Research 2019, 2019, 9.
[73] F. Ubaid, A. B. Radwan, N. Naeem, R. A. Shakoor, Z. Ahmad, M. F. Montemor, R. Kahraman, A. M. Abdullah, A. Soliman, Surface and Coatings Technology 2019, 372, 121.
[74] S. Saji Viswanathan, in *Corrosion Reviews*, Vol. 37, 2019, 187.
[75] F. Deflorian, S. Rossi, E. Scrinzi, Corrosion engineering, science and technology 2013, 48, 147.
[76] J. H. Xu, S. Ye, C. D. Ding, L. H. Tan, J. J. Fu, J. Mater. Chem. A 2018, 6, 5887.
[77] Y. Huang, L. Deng, P. Ju, L. Huang, H. Qian, D. Zhang, X. Li, H. A. Terryn, J. M. C. Mol, ACS Applied Materials & Interfaces 2018, 10, 23369.
[78] E. J. Brandon, M. Vozoff, E. A. Kolawa, G. F. Studor, F. Lyons, M. W. Keller, B. Beiermann, S. R. White, N. R. Sottos, M. A. Curry, D. L. Banks, R. Brocato, L. Zhou, S. Jung, T. N. Jackson, K. Champaigne, Acta Astronautica 2011, 68, 883.
[79] S. R. Zavada, N. R. McHardy, K. L. Gordon, T. F. Scott, ACS Macro Letters 2015, 4, 819.
[80] S. Liu, Z. Zheng, M. Li, X. Wang, Res. Chem. Intermed. 2012, 38, 1893; C. Ollivier, P. Renaud, Chem. Rev. 2001, 101, 3415.
[81] K. Biswas, D. Gilmer, N. Ghezawi, P.-F. Cao, T. Saito, Vacuum 2019, 164, 132.
[82] I. Yeo, H. Jung, T.-H. Song, Vacuum 2014, 104, 70.
[83] K. Biswas, Energies 2018, 11, 2228.
[84] R. C. R. Gergely, W. A. Santa Cruz, B. P. Krull, E. L. Pruitt, J. Wang, N. R. Sottos, S. R. White, Advanced Functional Materials 2018, 28, 1704197.
[85] K. A. Watson, F. L. Palmieri, J. W. Connell, Macromolecules 2002, 35, 4968; J. Chen, N. Ding, Z. Li, W. Wang, Progress in Aerospace Sciences 2016, 83, 37.
[86] M. R. Reddy, Journal of Materials Science 1995, 30, 281; H. R. Fischer, K. Tempelaars, A. Kerpershoek, T. Dingemans, M. Iqbal, H. v. Lonkhuyzen, B. Iwanowsky, C. Semprimoschnig, ACS Applied Materials & Interfaces 2010, 2, 2218; F. Rahmani, S. Nouranian, X. Li, A. Al-Ostaz, ACS Applied Materials & Interfaces 2017, 9, 12802.
[87] X. F. Lei, Y. Chen, H. P. Zhang, X. J. Li, P. Yao, Q. Y. Zhang, ACS Applied Materials & Interfaces 2013, 5, 10207.
[88] X. Wang, Y. Li, Y. Qian, H. Qi, J. Li, J. Sun, Advanced Materials 2018, 30, 1803854.
[89] E. Yousif, R. Haddad, Springerplus 2013, 2, 398.
[90] W. Guo, Y. Jia, K. Tian, Z. Xu, J. Jiao, R. Li, Y. Wu, L. Cao, H. Wang, ACS Applied Materials & Interfaces 2016, 8, 21046.
[91] D. Habault, H. Zhang, Y. Zhao, Chemical Society Reviews 2013, 42, 7244.
[92] L. Gao, J. He, J. Hu, C. Wang, ACS Applied Materials & Interfaces 2015, 7, 25546.
[93] L. Fang, J. Chen, Y. Zou, S. Chen, T. Fang, C. Lu, Z. Xu, Macromolecular Materials and Engineering 2017, 302, 1700059.
[94] Y.-K. Song, Y.-H. Jo, Y.-J. Lim, S.-Y. Cho, H.-C. Yu, B.-C. Ryu, S.-I. Lee, C.-M. Chung, ACS Applied Materials & Interfaces 2013, 5, 1378.
[95] C. P. Kabb, C. S. O'Bryan, C. C. Deng, T. E. Angelini, B. S. Sumerlin, ACS Applied Materials & Interfaces 2018, 10, 16793.
[96] J. Ling, M. Z. Rong, M. Q. Zhang, Polymer 2012, 53, 2691.
[97] Y. Wang, Q. Liu, J. Li, L. Ling, G. Zhang, R. Sun, C.-P. Wong, Polymer 2019, 172, 187.
[98] J. A. Carlson, J. M. English, D. J. Coe, Smart Mater. Struct. 2006, 15, N129.
[99] H. Zhang, Y. Zhao, ACS Applied Materials & Interfaces 2013, 5, 13069.

[100] Y. Bai, J. Zhang, D. Wen, P. Gong, J. Liu, J. Ju, X. Chen, Composites Science and Technology 2020, 187, 107940.
[101] S. Wu, J. Li, G. Zhang, Y. Yao, G. Li, R. Sun, C. Wong, ACS Appl. Mater. Interfaces 2017, 9, 3040.
[102] Y. Cheng, K. Ren, C. Huang, J. Wei, Sensors and Actuators B: Chemical 2019, 298, 126908.
[103] E. Borré, J.-F. Stumbé, S. Bellemin-Laponnaz, M. Mauro, Angew. Chem. Int. Ed. 2016, 55, 1313.
[104] H. Qin, T. Zhang, N. Li, H.-P. Cong, S.-H. Yu, Nature Communications 2019, 10, 2202.
[105] S.-L. Xiang, Q.-X. Hua, P.-J. Zhao, W.-L. Gong, C. Li, M.-Q. Zhu, Chem. Mater. 2019, 31, 5081.
[106] C. Lesaint, V. Risinggård, J. Hølto, H. H. Sæternes, H. Ø, S. Hvidsten, W. R. Glomm, "Self-healing high voltage electrical insulation materials", presented at *2014 IEEE Electrical Insulation Conference (EIC)*, 8-11 June 2014, 2014.
[107] C. W. Reed, S. W. Cichanowskil, IEEE Transactions on Dielectrics and Electrical Insulation 1994, 1, 904.
[108] K. Uchida, N. Shimizu, IEEE Transactions on Electrical Insulation 1991, 26, 271.
[109] Y. Zhang, H. Khanbareh, J. Roscow, M. Pan, C. Bowen, C. Wan, Matter 2020, 3, 989.
[110] S. Zwaag, *Self healing materials: an alternative approach to 20 centuries of materials science*, Vol. 30, Springer Science+ Business Media BV Dordrecht, The Netherlands, 2008.
[111] L. Gao, Y. Yang, J. Xie, S. Zhang, J. Hu, R. Zeng, J. He, Q. Li, Q. Wang, Matter 2020, 2, 451.
[112] S. Basu, I. German, R. Rhodes, G. C. Stevens, "Self-healing electrical insulation systems", presented at *2016 IEEE International Conference on Dielectrics (ICD)*, 3-7 July 2016, 2016.
[113] W. C. Röntgen, Annalen der Physik 1880, 247, 771.
[114] W. Yuan, L. Hu, S. Ha, T. Lam, G. Grüner, Q. Pei, *Self-clearable carbon nanotube electrodes for improved performance of dielectric elastomer actuators*, Vol. 6927, SPIE, 2008.
[115] S. Michel, B. T. T. Chu, S. Grimm, F. A. Nüesch, A. Borgschulte, D. M. Opris, J. Mater. Chem. 2012, 22, 20736.
[116] Y. Liu, M. Gao, S. Mei, Y. Han, J. Liu, Applied Physics Letters 2013, 103, 064101.
[117] S. Hunt, T. G. McKay, I. A. Anderson, Applied Physics Letters 2014, 104, 113701.
[118] E. Acome, S. K. Mitchell, T. G. Morrissey, M. B. Emmett, C. Benjamin, M. King, M. Radakovitz, C. Keplinger, Science 2018, 359, 61.
[119] N. Kellaris, V. Gopaluni Venkata, G. M. Smith, S. K. Mitchell, C. Keplinger, Science Robotics 2018, 3, eaar3276.
[120] C. Ellingford, R. Zhang, A. M. Wemyss, C. Bowen, T. McNally, Ł. Figiel, C. Wan, ACS Appl. Mater. Interfaces 2018, 10, 38438; Y. Zhang, C. Ellingford, R. Zhang, J. Roscow, M. Hopkins, P. Keogh, T. McNally, C. Bowen, C. Wan, Adv. Funct. Mater. 2019, 29, 1808431.
[121] C. Ellingford, R. Zhang, A. M. Wemyss, Y. Zhang, O. B. Brown, H. Zhou, P. Keogh, C. Bowen, C. Wan, ACS Appl. Mater. Interfaces 2020.
[122] C. Ellingford, A. M. Wemyss, R. Zhang, I. Prokes, T. Pickford, C. Bowen, V. A. Coveney, C. Wan, Journal of Materials Chemistry C 2020, 8, 5426.
[123] A. Shaaban, A. M. Schmidt, Smart Materials and Structures 2016, 25, 084018.
[124] M. Yoonessi, B. A. Lerch, J. A. Peck, R. B. Rogers, F. J. Solá-Lopez, M. A. Meador, ACS Applied Materials & Interfaces 2015, 7, 16932.
[125] A. S. Ahmed, R. V. Ramanujan, Journal of Materials Research 2015, 30, 946.
[126] M. Q. Zhang, M. Z. Rong, Journal of Polymer Science Part B: Polymer Physics 2012, 50, 229.
[127] E. Jeoffroy, D. Koulialias, S. Yoon, M. N. Partl, A. R. Studart, Construction and Building Materials 2016, 112, 497.
[128] E. Ogliani, L. Yu, I. Javakhishvili, A. L. Skov, RSC Advances 2018, 8, 8285.
[129] S. S. Bamji, A. T. Bulinski, Y. Chen, R. J. Densley, IEEE Transactions on Electrical Insulation 1992, 27, 402; N. Shimizu, C. Laurent, IEEE Transactions on Dielectrics and Electrical Insulation 1998, 5, 651; L. A. Dissado, S. J. Dodd, J. V. Champion, P. I. Williams, J. M. Alison, IEEE Transactions on Dielectrics and Electrical Insulation 1997, 4, 259.

[130] Y. Yang, J. He, Q. Li, L. Gao, J. Hu, R. Zeng, J. Qin, S. X. Wang, Q. Wang, Nature Nanotechnology 2019, 14, 151.
[131] F. Patti, K. Mansour, M. Pannirselvam, F. Giustozzi, Construction and Building Materials 2018, 171, 577.
[132] A. S. Ahmed, R. V. Ramanujan, Scientific Reports 2015, 5, 13773.
[133] E. D. Rodriguez, X. Luo, P. T. Mather, ACS Applied Materials & Interfaces 2011, 3, 152; X. Luo, P. T. Mather, ACS Macro Letters 2013, 2, 152.
[134] A. J. Bandodkar, C. S. López, A. M. Vinu Mohan, L. Yin, R. Kumar, J. Wang, 2016, 2, e1601465.
[135] Y. Liu, J. Yin, Y. Fu, P. Zhao, Y. Zhang, B. He, P. He, Chemical Engineering Journal 2020, 382, 122925.
[136] S. Efstathiou, A. M. Wemyss, G. Patias, L. Al-Shok, M. Grypioti, D. Coursari, C. Ma, C. J. Atkins, A. Shegiwal, C. Wan, D. M. Haddleton, Journal of Materials Chemistry B 2021, Advance Article.
[137] D. Zhang, S. Xu, X. Zhao, W. Qian, C. R. Bowen, Y. Yang, Advanced Functional Materials 2020, 30, 1910809.
[138] D. Zhang, K. Zhang, Y. Wang, Y. Wang, Y. Yang, Nano energy 2019, 56, 25; Y. Jiang, Y. Wang, H. Wu, Y. Wang, R. Zhang, H. Olin, Y. Yang, Nano-Micro Letters 2019, 11, 99; Y. Wang, Y. Wang, Y. Yang, Advanced Energy Materials 2018, 8, 1800961.
[139] C. Xu, R. Cui, L. Fu, B. Lin, Composites Science and Technology 2018, 167, 421.
[140] J. Cui, X. Li, Z. Pei, Y. Pei, Chemical Engineering Journal 2019, 358, 379.
[141] P. Puneet, R. Vedarajan, N. Matsumi, Electrochemistry Communications 2018, 93, 1.
[142] B. Ghosh, K. V. Chellappan, M. W. Urban, Journal of Materials Chemistry 2012, 22, 16104.
[143] Y. Zou, L. Fang, T. Chen, M. Sun, C. Lu, Z. Xu, Polymers 2018, 10, 474.
[144] F. I. Altuna, J. Antonacci, G. F. Arenas, V. Pettarin, C. E. Hoppe, R. J. J. Williams, Materials Research Express 2016, 3, 045003.
[145] Z. Wang, Y. Yang, R. Burtovyy, I. Luzinov, M. W. Urban, Journal of Materials Chemistry A 2014, 2, 15527.
[146] N. Yang, Z.-S. Wang, Z.-Y. Zhu, S.-C. Chen, G. Wu, Industrial & Engineering Chemistry Research 2018, 57, 14517.
[147] Z. Hu, Q. Shao, Y. Huang, L. Yu, D. Zhang, X. Xu, J. Lin, H. Liu, Z. Guo, Nanotechnology 2018, 29, 185602.

Received: ((will be filled in by the editorial staff))
Revised: ((will be filled in by the editorial staff))
Published online: ((will be filled in by the editorial staff))

Table of contents

Challenges and Opportunities of Self-healing Polymers and Devices for Extreme and Hostile Environments

James Ekeocha[1], Christopher Ellingford[1], Min Pan[2], Alan M Wemyss[1], Christopher Bowen[2], Chaoying Wan[1*]*

[1]International Institute for Nanocomposites Manufacturing (IINM), WMG, University of Warwick, CV4 7AL, UK

[2] Department of Mechanical Engineering, University of Bath, BA2 7AY, UK

Email: msscrb@bath.ac.uk ; chaoying.wan@warwick.ac.uk

Inspired by natural systems, a self-healing function provides exceptional advantages to enhance the robustness and stability of engineering materials, components and devices. This review considers self-healing in extreme or harsh environments such as those in space, deep ocean, and nuclear applications. The self-healing functions, operation mechanisms, challenges and opportunities are discussed.

ToC figure ((Please choose one size: 55 mm broad × 50 mm high **or** 110 mm broad × 20 mm high. Please do not use any other dimensions))